Linear Static and Dynamic Procedures for Structures with Velocity-Dependent Supplemental Dampers

Fahim Sadek
Bijan Mohraz
Michael A. Riley

ABSTRACT

Passive energy dissipation devices are used to reduce the damaging effects of earthquakes. These devices can absorb a portion of the earthquake-induced energy in structures and thus reduce the energy demand on structural members. Wide acceptance of these devices in structures will depend on the availability of simplified methods for their analysis and design.

The objectives of this study are: 1) to investigate the effect of increased viscous damping on the seismic response of structures; 2) to assess the accuracy of the linear static (LSP) and linear dynamic (LDP) procedures recommended in the NEHRP Guidelines for the Seismic Rehabilitation of Buildings (FEMA 273) for design of structures with velocity-dependent passive energy dissipation devices; and 3) to propose modifications to the current design procedures to improve their accuracy and reliability. Based on the analysis of single-degree-of-freedom structures under an ensemble of earthquake records, it is shown that the effect of increased damping on the displacement response is more pronounced in structures with intermediate periods. For long-period structures, however, an increase in damping decreases displacements, but increases the absolute accelerations and consequently, the seismic forces. The study also identifies the following limitations of the FEMA 273 procedures: 1) the use of a constant reduction factor for the displacement response of short-period structures; 2) the assumption of a harmonic response to compute the peak velocity; and 3) the computation of design forces based on the assumption that the structure undergoes a harmonic motion with an amplitude equal to the peak displacement and a frequency equal to that of the fundamental mode. In most cases, these assumptions result in non-conservative estimates of the peak response and design force. Comparisons of the methods proposed in this study and in FEMA 273 for several single- and multi-degree-of-freedom structures indicate that the former produces more reliable results.

Keywords: Building technology; design codes; passive energy dissipation; supplemental dampers; structural control; structural dynamics.

ACKNOWLEDGMENTS

TABLE OF CONTENTS

LIST OF TABLES

LIST OF FIGURES

1. INTRODUCTION

The advantages of damping in structures have long been recognized and accepted. Inherent equivalent viscous damping in the range of 2 % to 5 % of critical damping has been generally used in the analysis and design of structures subjected to dynamic loads such as earthquakes and wind. For example, in seismic codes and provisions, design spectra are usually given for 5 % of critical damping. In recent years, several passive techniques utilizing supplemental damping mechanisms have been introduced to enhance the damping capacity of structures and reduce the damage from earthquakes. These techniques include seismic isolation and supplemental damping devices. In the former, the structure is mounted on flexible elements such as elastomeric or sliding friction bearings to shift the natural vibration period of the structure beyond that of the earthquake excitation, while a damping mechanism is provided to control the deflection across the isolation interface. In the latter, supplemental dampers are attached to the structure, usually to its bracing system, to increase its energy absorbing capacity.

Supplemental dampers, also known as passive energy dissipation devices, can absorb a portion of earthquake-induced energy in the structure and reduce the energy demand on the primary structural members such as beams, columns, beam-column joints, and walls. These devices can substantially reduce the inter-story drifts and consequently, nonstructural damage. The NEHRP Guidelines for the Seismic Rehabilitation of Buildings (FEMA 273) categorize these devices according to their mechanical behavior as:

1. Displacement-dependent devices: The force-displacement response characteristics of these devices are primarily a function of the relative displacement rather than the relative velocity between the ends of the device. This category includes friction devices that exhibit rigid-plastic behavior (box-like hysteresis), and metallic yielding devices that exhibit hysteretic behavior that can be approximated as bilinear or trilinear.
2. Velocity-dependent devices: The force-displacement response characteristics of these devices are primarily a function of the relative velocity between the ends of the device or the frequency of motion. This category includes solid viscoelastic (constrained layers of acrylic polymers deforming primarily in shear), fluid viscoelastic (viscous shear walls), and fluid viscous (fluid flow through orifices) devices. The forces, $F(t)$, generated by the devices in this category can generally be expressed as

$$F(t) = K_{eff}\Delta(t) + C\dot{\Delta}(t) \tag{1.1}$$

where $\Delta(t)$ and $\dot{\Delta}(t)$ are the relative displacement and velocity, respectively, between the ends of the device, K_{eff} is the effective stiffness, and C is the damping coefficient of the device. For further details, one should refer to Chapter 9 of the NEHRP Guidelines (FEMA 273) and the commentary (FEMA 274).

3. Other devices: Several devices have been developed that cannot be classified as either displacement- or velocity-dependent. This category includes shape memory alloys and fluid-restoring force/damping devices.

Wide acceptance of passive energy dissipation devices in structures will depend on the availability of simplified methods for their analysis and design. FEMA 273 guidelines present linear static and dynamic procedures as well as the more sophisticated nonlinear static and dynamic procedures for analysis of rehabilitated structures incorporating these devices. As will be demonstrated later, the FEMA 273 procedures have the following shortcomings which usually result in a non-conservative design: 1) the use of a constant reduction factor for computing the displacement response of short-period structures; 2) the assumption of a harmonic response for computing the peak velocity; and 3) the computation of design forces assuming that the structure undergoes a harmonic motion with an amplitude equal to the peak displacement and a frequency equal to that of the fundamental mode. This study is concerned with investigating the influence of velocity-dependent supplemental dampers on the seismic response of structures, evaluating the accuracy of the linear static and dynamic procedures presented in FEMA 273, and proposing modifications to these procedures for the analysis of structures with velocity-dependent dampers.

This report briefly reviews studies on the influence of supplemental viscous damping on the seismic response of structures as well as methods of analysis and design presented in recent seismic codes and provisions such as the UBC code and the NEHRP recommended provisions. Analyses of several single-degree-of-freedom (SDOF) structures with different damping ratios under a large number of earthquake excitations are carried out. The results of the statistical analysis are used in developing linear static and dynamic procedures for design of structures with linearly elastic behavior and velocity-dependent dampers. The proposed method is used in the analysis of several single- (SDOF) and multi-degree-of-freedom (MDOF) structures. The method proposed in this study is compared with that recommended in FEMA 273 and with time history analyses to illustrate the accuracy of the proposed method.

2. SUMMARY OF PREVIOUS WORK

The influence of increased viscous damping on the seismic response of structures has been studied by a number of investigators. Newmark and Hall (1982) presented the effect of damping ratio, β, in the range of 0.5 % to 20 % on the median (50 percentile) amplification in the three spectral regions (acceleration, velocity, and displacement) as:

$$\begin{aligned}
\text{Acceleration amplification} &= 3.21 - 0.68 \ln 100\beta \\
\text{Velocity amplification} &= 2.31 - 0.41 \ln 100\beta \\
\text{Displacement amplification} &= 1.82 - 0.27 \ln 100\beta
\end{aligned} \tag{2.1}$$

The effect of inherent and supplemental damping on the earthquake spectral displacement, SD, has been studied by Ashour and Hanson (1987) who proposed a relationship describing the decrease in SD with the increase in β. They used SDOF structures with natural periods, T, from 0.5 s to 3.0 s in increments of 0.5 s, and damping ratios of 0 %, 2 %, 5 %, 10 %, 20 %, 30 %, 50 %, 75 %, 1.00 % (critically damped), 125 %, and 150 %. The excitations consisted of three actual and twelve artificial accelerograms. The computed spectral displacement for each period was normalized to those for zero and 5 % damping ratios for each record. The results of their statistical analysis led to the introduction of a reduction factor, r_f, which for normalization to zero damping is given as:

$$r_f = \sqrt{\frac{1 - e^{-\beta B}}{\beta B}} \tag{2.2}$$

and for normalization to 5 % damping as:

$$r_f = \sqrt{0.05 \frac{1 - e^{-\beta B}}{\beta(1 - e^{-0.05B})}} \tag{2.3}$$

where B is a parameter that ranges from 24 (upper bound) to 140 (lower bound) for normalization to zero damping and from 18 (upper bound) to 65 (lower bound) for normalization to 5 % damping. The equations reflect the decaying pattern of the spectral displacement with the increase in the damping ratio.

Since structures experience nonlinear behavior under strong earthquake excitations, it is important to determine the effect of increased damping on the inelastic response of structures. Wu and Hanson (1989) studied the elastic-plastic response of SDOF systems with large damping and different ductilities. They selected structures with two periods in the acceleration region ($T = 0.1$ s and 0.5 s), one period in the velocity region ($T = 0.5$ s to 3.0 s)[*], and two periods in the displacement region ($T = 3.0$ s and 10.0s) with damping ratios, β, of

---

[*] In the velocity region, the spectra were approximated by parabolas between periods of 0.5 s to 3.0 s and the statistical analysis was performed on the peaks of the parabolas.

3

10 %, 20 %, 30 %, and 50 %; and ductility ratios, μ, of 1, 1.5, 2, 3, 4, and 6. The excitations included nine actual and one artificial accelerograms. The results of the statistical analysis indicated that the response amplification, Ψ, (response parameter divided by the corresponding peak ground motion) at each period can be estimated from the following equation:

$$(\beta, \mu) = p\, ln(q\beta)[r\mu - (r-1)]^s \qquad (2.4)$$

where p, q, r, and s are constants for the given periods, see Table 2.1. Amplifications for other periods may be obtained by linear interpolation. The study indicated that the effect of damping on the inelastic response is similar to its effect on the elastic response. For the elastic case, normalization to the response for a damping ratio of β_0 results in a reduction factor of

$$r_f = \frac{\ln q\beta}{\ln q\beta_0} \qquad (2.5)$$

Comparisons of the results obtained by Ashour and Hanson (1987) and those by Wu and Hanson (1989) for $\mu = 1$ indicate close agreement (Hanson et al., 1993).

Table 2.1. Numerical Factors Used in Equation (2.4)
(After Wu and Hanson, 1989)

Period (s)	p	q	r	s
0.1	-0.35	0.10	2.9	-0.24
0.5	-0.55	0.42	1.8	-0.56
0.5 to 3	-0.47	0.52	1.5	-0.7
3	-0.48	0.48	1.0	-1.0
10	-0.29	0.05	1.0	-1.0

The studies by Newmark and Hall (1982), Ashour and Hanson (1987), and Wu and Hanson (1989) indicate similar conclusions regarding the reductions in earthquake spectral displacements with an increase in viscous damping. No consideration, however, was given to the influence of increased damping on the absolute acceleration response which, as discussed later, is the key parameter for computing the seismic forces and base shears in structures with passive energy dissipation devices.

4

3. SEISMIC CODES AND PROVISIONS

Recent seismic codes and provisions include the influence of supplemental damping on design forces and displacements. For base isolated structures, the Uniform Building Code (UBC 1994 and 1997) and the NEHRP Recommended Provisions for Seismic Regulations for New Buildings (NEHRP 1994 and 1997) specify that the design displacement of the isolation system be computed by dividing the 5 % damped elastic response by a factor that depends on the damping in the system. This factor is equal to 0.8, 1.0, 1.2, 1.5, 1.7, 1.9, and 2.0 for effective viscous damping ratios of $\leq$ 2 %, 5 %, 10 %, 20 %, 30 %, 40 %, and $\geq$ 50 %, respectively. The seismic forces are estimated by multiplying the computed isolator displacement by the maximum effective stiffness of the isolation system.

The 1994 NEHRP provisions provided, in an appendix to Chapter 2, a method for computing the design forces for structures with viscous dampers with damping ratios less than or equal to 30 %. The procedure is to multiply the design forces computed for a 5 % damped spectrum by a reduction factor of 1.00, 0.84, 0.72, 0.64, 0.58, and 0.53 for damping ratios of 5 %, 10 %, 15 %, 20 %, 25 %, and 30%, respectively, regardless of the period of the structure. The provisions also introduced a method for computing the equivalent damping ratio of a structure with viscous dampers. For damping ratios greater than 30 %, a time history analysis should be used.

The NEHRP Guidelines for the Seismic Rehabilitation of Buildings (FEMA 273) present a method for constructing design spectra for a given damping from the 5 % damped spectra. The procedure is to divide the spectral ordinates in the constant acceleration and constant velocity regions by a factor, B_s and B_1, respectively, corresponding to the specified damping ratio. These factors, which are based on the recommendations of Newmark and Hall (1982), are presented in Table 3.1 where it is observed that the factors in the velocity region are the same as those recommended for base isolation in the 1994 and 1997 UBC and NEHRP provisions. For base isolated structures, FEMA 273 recommends using the same procedure in the 1994 and 1997 UBC and NEHRP provisions to compute the design displacement of the isolator by dividing the 5 % damped displacement by the factor for the velocity region.

FEMA 273 presents the first comprehensive method of analysis and design for structures with passive energy dissipation devices. The guidelines recommend the use of a simplified linear static procedure (LSP) or a linear dynamic procedure (LDP) for structures with linear behavior and with displacement- and velocity-dependent passive energy dissipation devices. In addition, for structures with nonlinear behavior, the guidelines recommend a nonlinear static (NLSP) or a nonlinear dynamic (NLDP) procedure.

The two linear procedures are limited to structures with a framing system, exclusive of the energy dissipation devices, that remains essentially linearly elastic for the expected level of seismic demand. In addition, the effective damping afforded by the energy dissipation shall not exceed 30 % of critical in the fundamental mode. The LSP and LDP can be summarized as follows:

5

Table 3.1. Damping Factors as a Function of Viscous Damping Ratio
(After FEMA 273)

Damping Ratio β	Damping Factors	
	Acceleration Zone B_s	Velocity Zone B_1
≤2	0.8	0.8
5	1.0	1.0
10	1.3	1.2
20	1.8	1.5
30	2.3	1.7
40	2.7	1.9
≥50	3.0	2.0

1. Assume the effective damping ratio, β_{eff}, in the fundamental mode (LSP) or the first significant modes (LDP).

2. Use the factors B_s or B_1 in Table 3.1 to reduce the base shear for 5 % damping (LSP) or the spectral acceleration for 5 % damping (LDP) and then distribute the forces along the height of the structure (LSP) using the method presented in the guidelines for conventional structures (without energy dissipation devices).

3. Analyze the structure using any analytical method (LSP) or modal superposition method (LDP) to compute the design displacements. Calculate the effective damping ratio, β_{eff}, using the method outlined in FEMA 273 and iterate on steps 1 through 3 until convergence is achieved.

4. Assuming a harmonic response, compute the velocity between the damper ends by multiplying the displacements by the fundamental frequency (LSP) or by multiplying the modal displacements by the modal frequencies (LDP). Calculate the damper forces as the product of the damping coefficient and the relative velocity.

5. Compute design forces as the maximum of the following distinct stages of deformation:

   - at maximum drift: where the forces are computed as in step 2,
   - at maximum velocity and zero drift: where only the viscous forces in the dampers are applied to the structure, and
   - at maximum floor acceleration: where the forces are computed as the sum of the forces at maximum drift times CF_1 and the forces at maximum velocity times CF_2. CF_1 and CF_2 are functions of the effective damping ratio, β_{eff}, such that:

$$CF_1 = \cos[\tan^{-1}(2\beta_{eff})] \qquad CF_2 = \sin[\tan^{-1}(2\beta_{eff})] \qquad (3.1)$$

The procedure presented in FEMA 273 implies that the design forces are computed using the peak restoring forces for displacements that are reduced due to the influence of the supplemental damping. In order to account for the forces in the dampers, a check is

performed at the stages of maximum velocity and maximum acceleration where the structure is assumed to undergo a harmonic motion at the fundamental frequency (LSP) or at each modal frequency (LDP) with an amplitude corresponding to the maximum drift. See also Whittaker et al. (1996 and 1997) and Tsopelas et al. (1997) for more details.
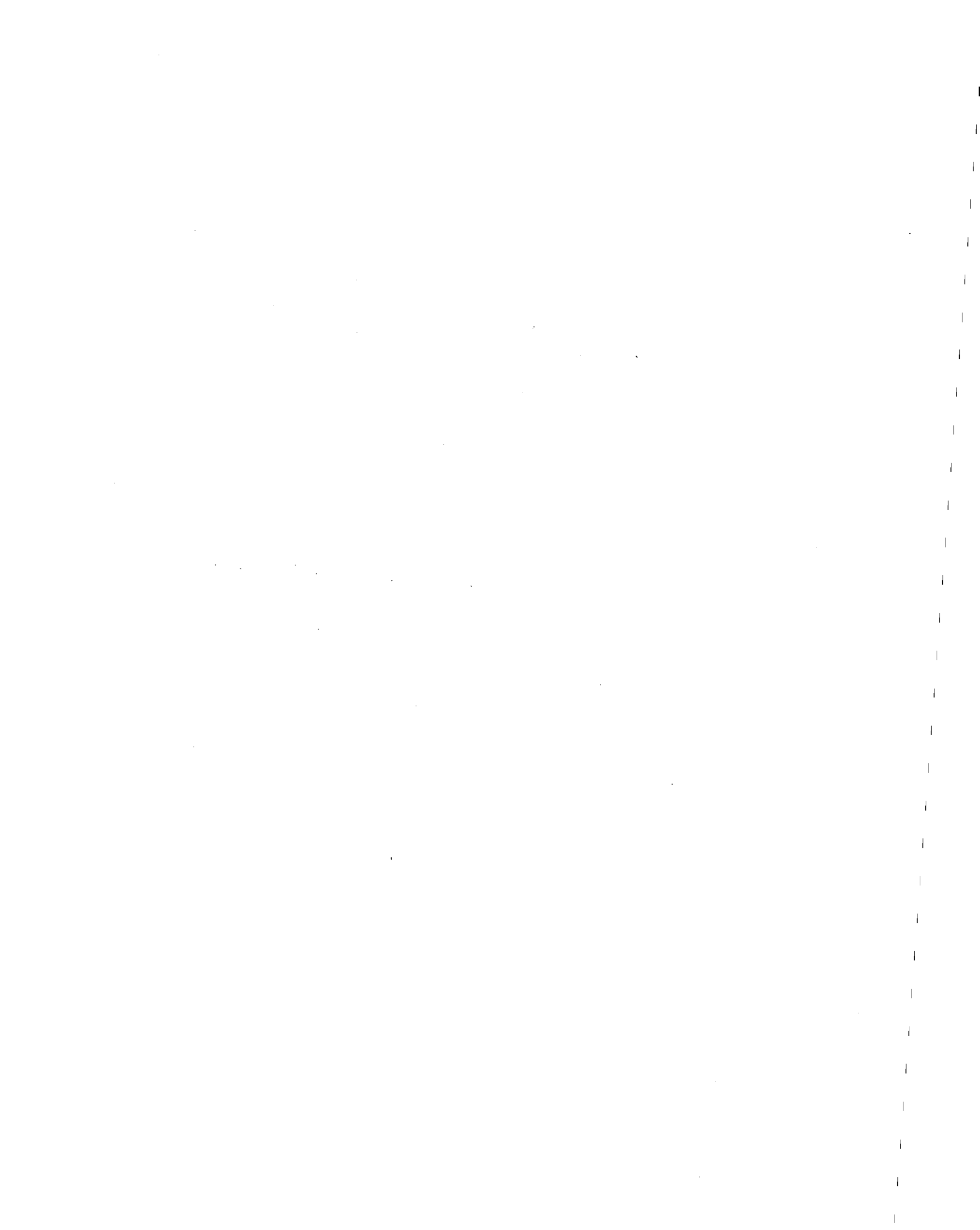
4. ANALYSIS

The reduction factors presented by Newmark and Hall (1982), Ashour and Hanson (1987), and Wu and Hanson (1989) can be used to modify the displacement response or drifts of structures with supplemental dampers. They cannot, however, be used to compute the seismic design forces or base shears. The reason is given in the following paragraphs.

For a conventional structure (a structure without supplemental dampers) modeled as a SDOF with mass m, damping c, and stiffness k subjected to an earthquake excitation, the equation of motion is given by:

$$m\ddot{x}_t(t) + c\dot{x}(t) + kx(t) = 0 \tag{4.1}$$

where $\ddot{x}_t(t)$ is the absolute acceleration which is equal to $\ddot{x}(t) + \ddot{x}_g(t)$, while $x(t)$, $\dot{x}(t)$, and $\ddot{x}(t)$ are the relative displacement, velocity, and acceleration, respectively; and $\ddot{x}_g(t)$ is the ground acceleration. The practice has been to compute the maximum base shear, V, as the peak force in the spring which is equal to (Chopra, 1995):

$$V = k|x(t)|_{max} = k\,SD = m\omega^2\,SD = m\,PSA \tag{4.2}$$

where ω is the natural frequency and PSA is the pseudo-acceleration equal to $\omega^2\,SD$. For the case where the SDOF structure is equipped with a supplemental damper, the base shear is the sum of the forces in the spring and damper. Therefore,

$$V = |kx(t) + c\dot{x}(t)|_{max} = |m\ddot{x}_t(t)|_{max} = m\,SA \tag{4.3}$$

where c in Equation (4.3) represents the sum of inherent and supplemental damping coefficients. For this case, the base shear is equal to the mass times the peak absolute acceleration SA rather than the pseudo-acceleration PSA. It should be noted that, for zero damping, PSA is equal to SA and for small damping ratios (up to 10 %), the two are approximately equal and may be used interchangeably. For larger damping ratios, however, the difference between PSA and SA is significant and the pseudo-acceleration cannot be used as the absolute acceleration. Therefore, when computing the base shear for structures with supplemental dampers with large damping ratios, the absolute acceleration response must be used, and the reduction factors presented earlier which are based on the spectral displacement (or pseudo spectral acceleration) can only be used to reduce drifts but not to compute forces.

To investigate the effect of the damping ratio on the relative displacement and absolute acceleration response of structures, linear SDOF systems with periods ranging from 0.1 s to 4.0 s with increments of 0.1 s and damping ratios of 2 %, 5 %, 10 %, 15 %, 20 %, 30 %, 40 %, 50 %, and 60 % of critical were considered in this study. The structures were subjected to a set of 72 horizontal components of accelerograms from 36 stations in the western Unites States (see Appendix A). These records include a wide range of earthquake

magnitudes (5.2 to 7.7), epicentral distances (6 km to 127 km), peak ground accelerations (0.044 g to 1.172 g), and soil conditions. The relative displacement and absolute acceleration response ratios are computed as the ratio of the peak response of the structure with different damping ratios to the peak response with a damping ratio of 5 %. The responses were normalized to those for 5 % damping since design spectra in seismic codes are normally presented for this damping. The mean displacement and acceleration ratios for the 72 records are presented in Figures 4.1 and 4.2, respectively. Typical mean ± standard deviation values associated with the computed response ratios are presented in Appendix B. Figures 4.1 and 4.2 show that increasing the supplemental damping results in a further reduction in the displacement response. The effect of damping is more pronounced in the velocity region (structures with mid-range periods). While larger damping ratios (greater than approximately 40 %) provide further reductions in the displacement response, the additional reductions are not significant and the increased damping adversely affects the absolute acceleration response and consequently, the seismic forces, especially for long-period (flexible) structures.

Since forces in viscous dampers depend on the relative velocity, it is important to study the effect of increased damping on the relative velocity response of structures. In this study, for each record, the peak relative velocity (or spectral velocity), SV, was computed for different periods and damping ratios and divided by the pseudo-velocity, PSV ($PSV = \omega\, SD$). From the mean values of $SV / \omega\, SD$ for the 72 accelerograms, Figure 4.3, it may be concluded that assuming the peak relative velocity to be equal to the pseudo-velocity (harmonic response) is valid only for periods in the neighborhood of 0.5 s. For shorter periods, the peak velocity is smaller than the pseudo-velocity while for longer periods, the peak velocity is larger and increases as the period and damping ratio increase.

Figure 4.4 presents a comparison of the displacement reduction factors computed from this study and those from the studies by Newmark and Hall (1982) and Wu and Hanson (1989) for damping ratios of 10 %, 20 %, 30 % and 50 %. The figure indicates that for the three studies, the reduction factors fall within a narrow range in the mid- to long-period region. Similar to the study by Wu and Hanson (1989), this study shows that, for the short period range (periods less than 0.5 s), the reduction factors vary significantly and are larger for shorter periods. The study by Newmark and Hall (1982) which is used to reduce design spectra in FEMA 273 does not reflect this behavior.
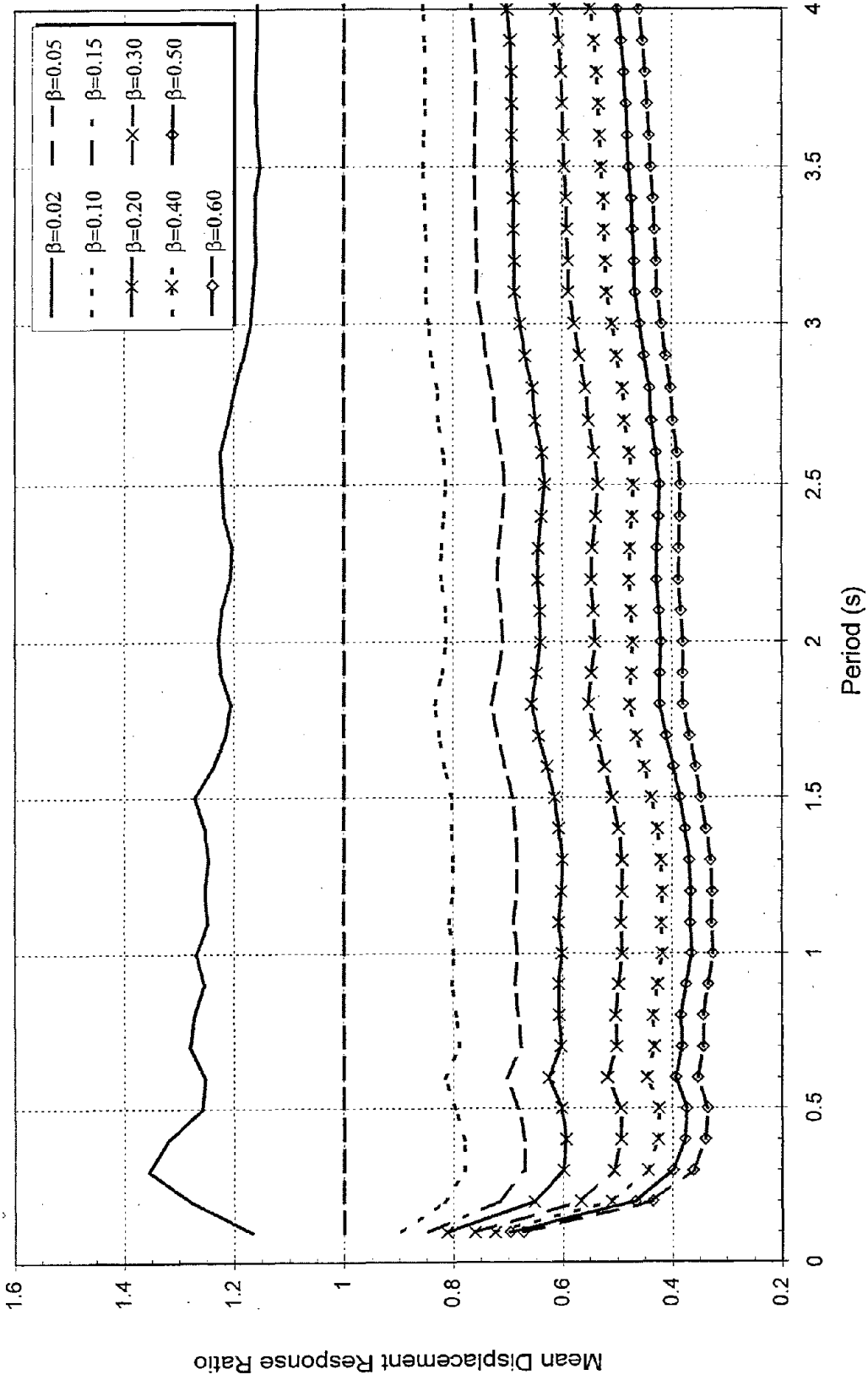
Figure 4.1. Mean Displacement Response Ratios for SDOF Structures with Supplemental Damping

11
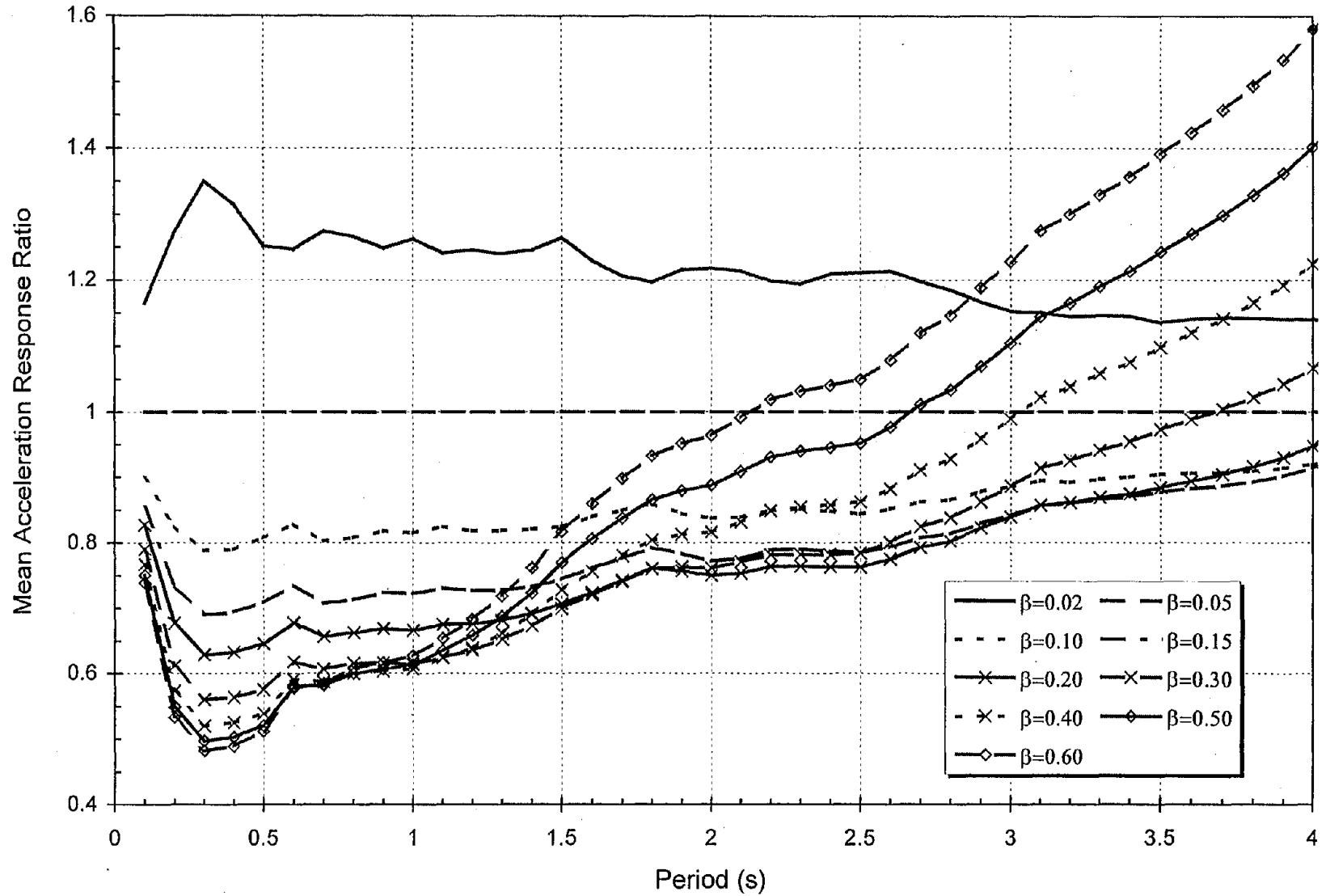
Figure 4.2. Mean Acceleration Response Ratios for SDOF Structures with Supplemental Damping
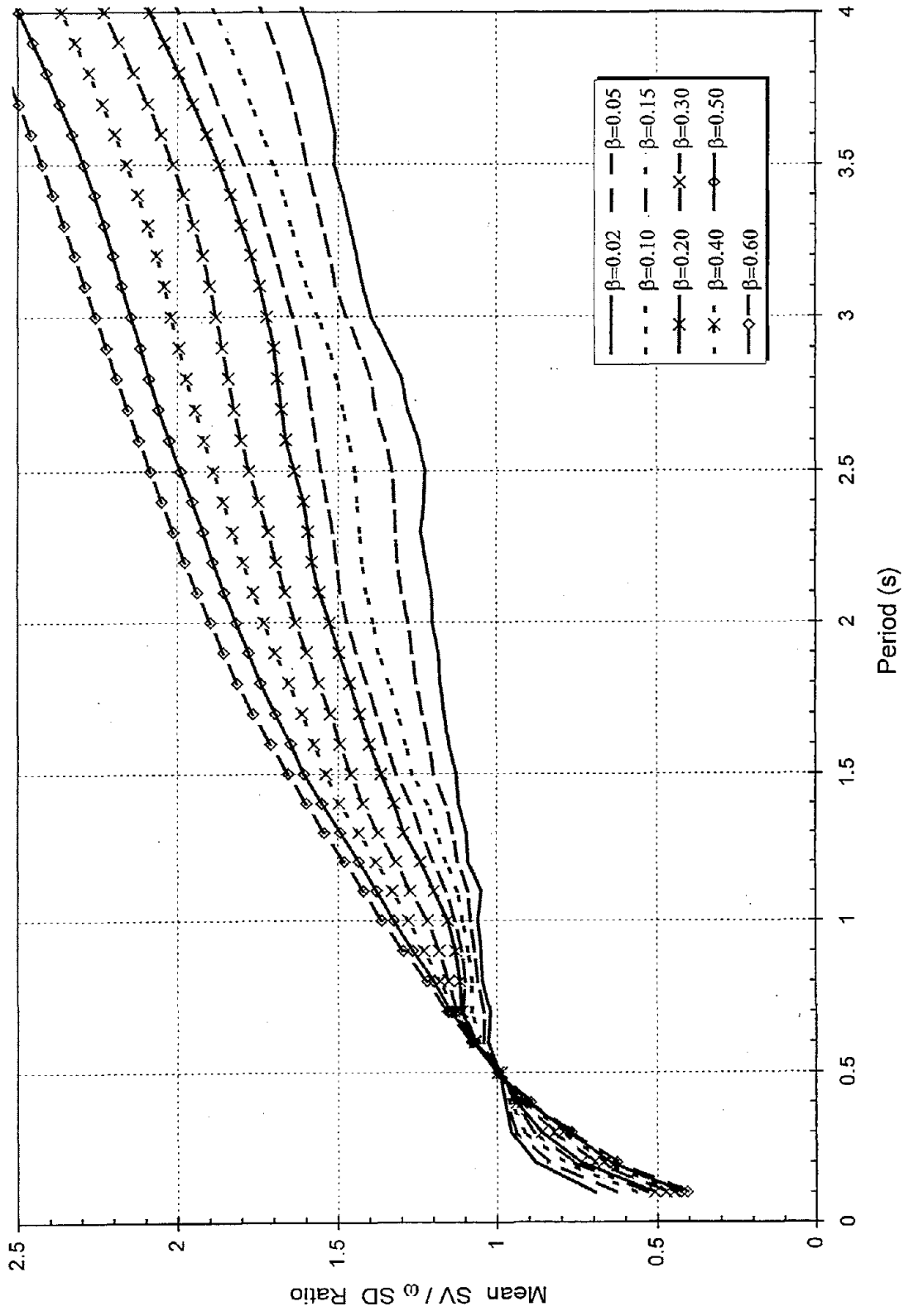
Figure 4.3. Mean Spectral Velocity to Pseudo-Velocity Ratios for SDOF Structures with Supplemental Damping

13
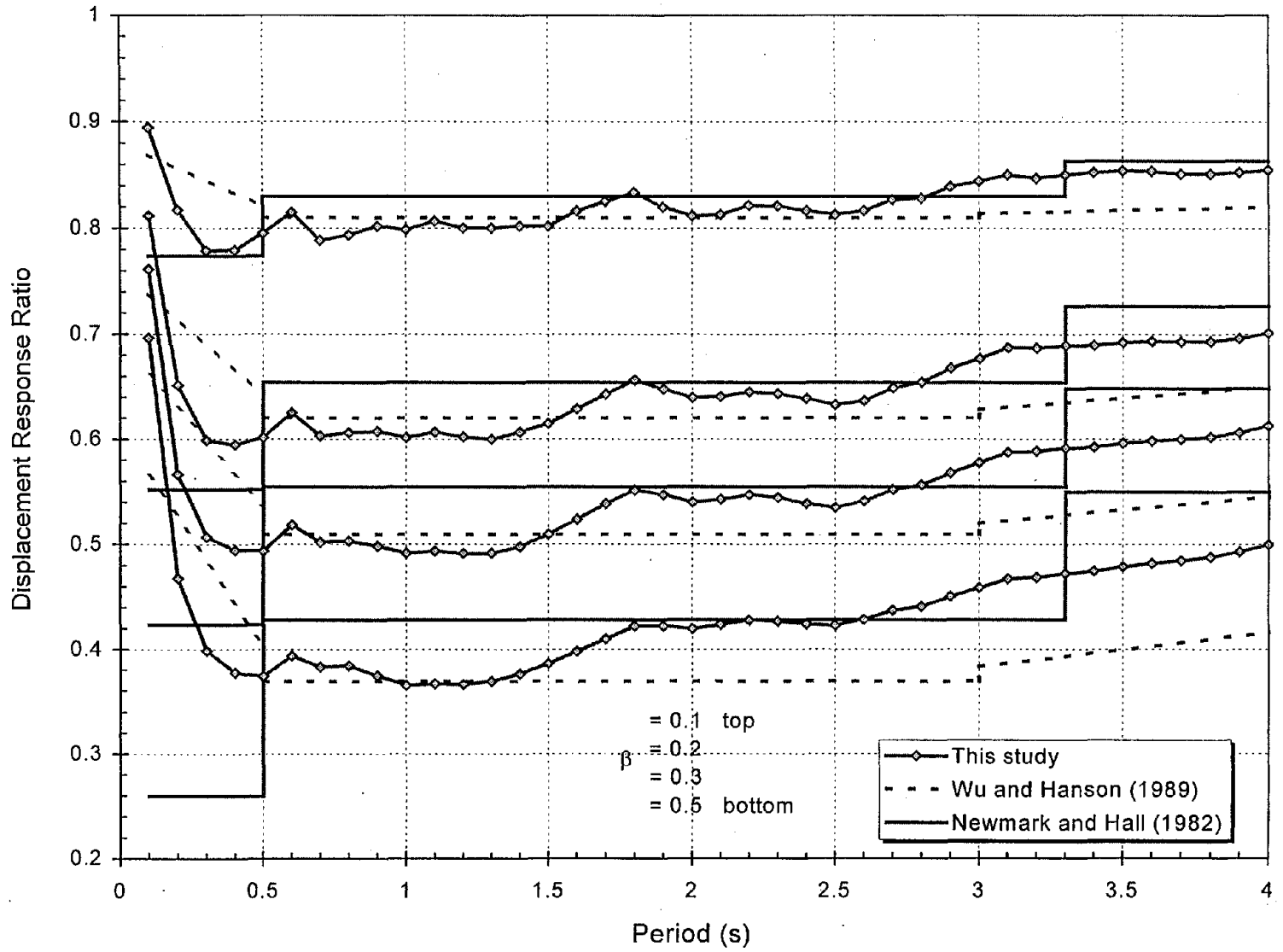
Figure 4.4. Comparison between Displacement Reduction Factors Using Different Methods

5. PROPOSED PROCEDURES

As discussed in previous sections, computing the story shears from the restoring forces only or assuming the seismic response to be harmonic (i.e. the velocity is equal to the product of natural frequency and displacement) is not accurate, especially for structures with large damping ratios. Based on the analysis presented in the previous section, a more reliable method for design of structures with velocity-dependent supplemental dampers is introduced in this section. The method can be used with the linear static or the linear dynamic procedures.

In the proposed procedure, three damping factors are introduced: a displacement factor, α_d, that can be used to reduce displacements and drifts, a force factor, α_a, that can be used to amplify or attenuate the design forces and base shears, and a velocity factor, α_v, that can be used to compute relative velocities. The displacement, force, and velocity factors which are based on Figures 4.1 to 4.3 are presented for selected periods in Tables 5.1 to 5.3. The tables show that for small damping ratios (up to 10 %), the displacement factors are very close to the force factors. For large damping ratios, the force factors are larger than the displacement factors. The difference between the two is more pronounced at longer periods.

Table 5.1. Displacement Damping Factors α_d

Period	Viscous Damping Ratio β								
(s)	0.02	0.05	0.10	0.15	0.20	0.30	0.40	0.50	0.60
0.1	1.17	1	0.89	0.85	0.81	0.76	0.72	0.70	0.67
0.3	1.35	1	0.78	0.67	0.60	0.51	0.44	0.40	0.36
0.5	1.26	1	0.80	0.68	0.60	0.49	0.42	0.37	0.34
1.0	1.27	1	0.80	0.68	0.60	0.49	0.42	0.36	0.33
1.5	1.27	1	0.80	0.69	0.61	0.51	0.44	0.39	0.35
2.0	1.23	1	0.81	0.71	0.64	0.54	0.47	0.42	0.38
2.5	1.22	1	0.81	0.71	0.63	0.53	0.47	0.42	0.38
3.0	1.17	1	0.84	0.75	0.68	0.58	0.51	0.46	0.42
3.5	1.15	1	0.85	0.76	0.69	0.60	0.53	0.48	0.44
4.0	1.16	1	0.85	0.77	0.70	0.61	0.55	0.50	0.46

15

Table 5.2. Force Damping Factors α_a

Period (s)	Viscous Damping Ratio β								
	0.02	0.05	0.10	0.15	0.20	0.30	0.40	0.50	0.60
0.1	1.16	1	0.90	0.86	0.83	0.79	0.77	0.75	0.74
0.3	1.35	1	0.79	0.69	0.63	0.56	0.52	0.50	0.48
0.5	1.25	1	0.81	0.71	0.65	0.57	0.54	0.52	0.51
1.0	1.26	1	0.82	0.72	0.67	0.61	0.61	0.61	0.63
1.5	1.26	1	0.82	0.74	0.71	0.70	0.73	0.77	0.82
2.0	1.22	1	0.84	0.77	0.75	0.76	0.82	0.89	0.96
2.5	1.21	1	0.84	0.78	0.76	0.78	0.86	0.95	1.05
3.0	1.15	1	0.89	0.84	0.84	0.89	0.99	1.10	1.23
3.5	1.14	1	0.90	0.88	0.88	0.97	1.10	1.24	1.39
4.0	1.14	1	0.92	0.91	0.95	1.07	1.23	1.40	1.58

Table 5.3. Velocity Damping Factors α_v

Period (s)	Viscous Damping Ratio β								
	0.02	0.05	0.10	0.15	0.20	0.30	0.40	0.50	0.60
0.1	0.70	0.63	0.57	0.53	0.51	0.47	0.45	0.43	0.41
0.3	0.96	0.94	0.91	0.88	0.86	0.82	0.79	0.78	0.77
0.5	0.99	0.99	0.99	0.99	0.99	1.00	1.00	1.00	1.00
1.0	1.06	1.08	1.11	1.13	1.15	1.22	1.28	1.32	1.36
1.5	1.13	1.20	1.27	1.31	1.36	1.46	1.54	1.61	1.65
2.0	1.20	1.28	1.39	1.47	1.53	1.63	1.73	1.82	1.90
2.5	1.23	1.33	1.47	1.55	1.64	1.78	1.89	1.99	2.09
3.0	1.39	1.47	1.56	1.64	1.72	1.88	2.02	2.15	2.26
3.5	1.51	1.60	1.70	1.79	1.87	2.01	2.16	2.29	2.42
4.0	1.61	1.74	1.88	2.00	2.09	2.23	2.36	2.50	2.62

These factors may be used in design as follows: for the structure without supplemental dampers, compute the base shear (LSP) or the spectral acceleration (LDP) from the 5 % damped design spectrum and compute the floor displacements, inter-story drifts, and story shears as usual. Multiply the displacements and drifts by the displacement factor α_d to determine the actual deformations, multiply the story shears by the force factor α_a to compute the actual forces and the base shear, and compute the damper forces as the damping coefficient times the relative velocities which are computed as the product of the relative displacement, natural frequency, and velocity factor α_v.

Although simple, the above method does not explicitly include the contribution of the damper forces in the computation of design forces and base shear. Therefore, erroneous results may be expected especially for multi-story frames with non-uniform distribution of

dampers. Consequently, another method is presented in this study. The method is parallel to that in FEMA 273 which includes the influence of the damper forces on the computed design actions directly; thereby, accounting for the distribution of the dampers along the height of the building.

The method assumes that the velocity-displacement response in the quadrant having the absolute peak displacement, SD, and absolute peak velocity, SV, can be approximated by an ellipse. To examine the accuracy of this assumption, the responses of four SDOF structures to the S00E component of El Centro, the Imperial Valley earthquake of 1940 and the N21E component of Taft Lincoln School Tunnel, the Kern County earthquake of 1952 were computed. The structures had periods of 0.2 s and 2.0 s, each with a damping ratio of 10 % and 30 %. The velocity-displacement responses of the structures are plotted in Figures 5.1 and 5.2 for the first 12 s of the El Centro and Taft records, respectively, along with the assumed elliptical peak velocity-displacement response. The figures show that the assumption of an elliptical velocity-displacement response is a good approximation for a short-period structure and a reasonable approximation for a long-period structure. The velocity-displacement relationship, thus, can be expressed as:

$$\left(\frac{x(t)}{SD}\right)^2 + \left(\frac{\dot{x}(t)}{SV}\right)^2 = 1 \tag{5.1}$$

Substituting for $SV = \alpha_v \omega SD$ as discussed earlier, Equation (5.1) takes the form:

$$\left(x(t)\right)^2 + \left(\frac{\dot{x}(t)}{\alpha_v \omega}\right)^2 = SD^2 \tag{5.2}$$

Maximizing the design force $F(t) = kx(t) + c\dot{x}(t)$ subject to the constraint of Equation (5.1) will result in the peak forces at the stage of maximum acceleration given as:

$$V = C_1 k SD + C_2 c SV = C_1 F_d + C_2 F_v \tag{5.3}$$

where F_d and F_v are the forces at maximum drift and velocity, respectively, and C_1 and C_2 are given by:

$$C_1 = \frac{F_d}{\sqrt{F_d^2 + F_v^2}} \tag{5.4}$$
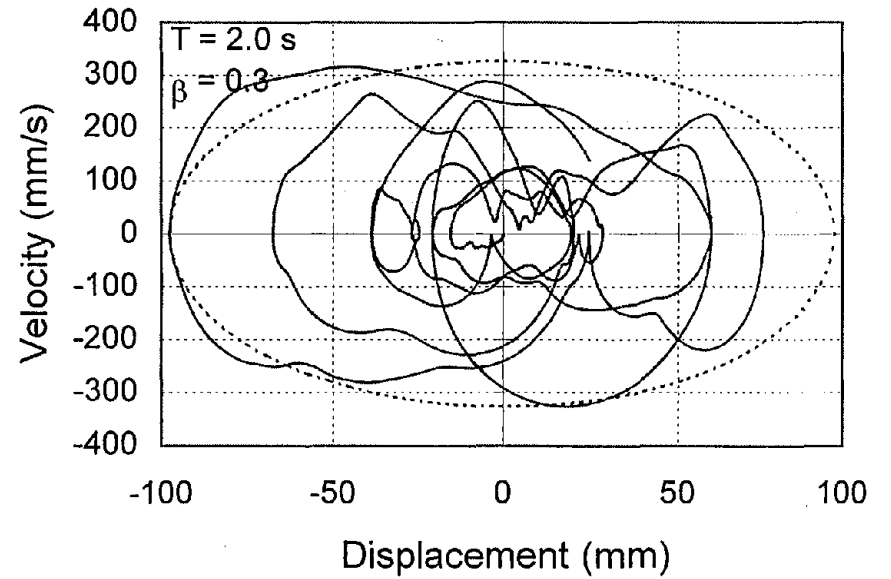
and

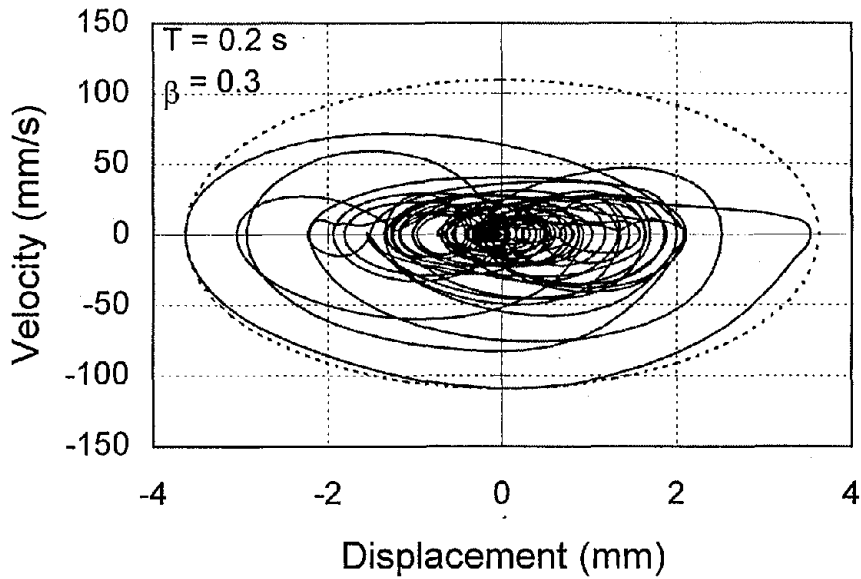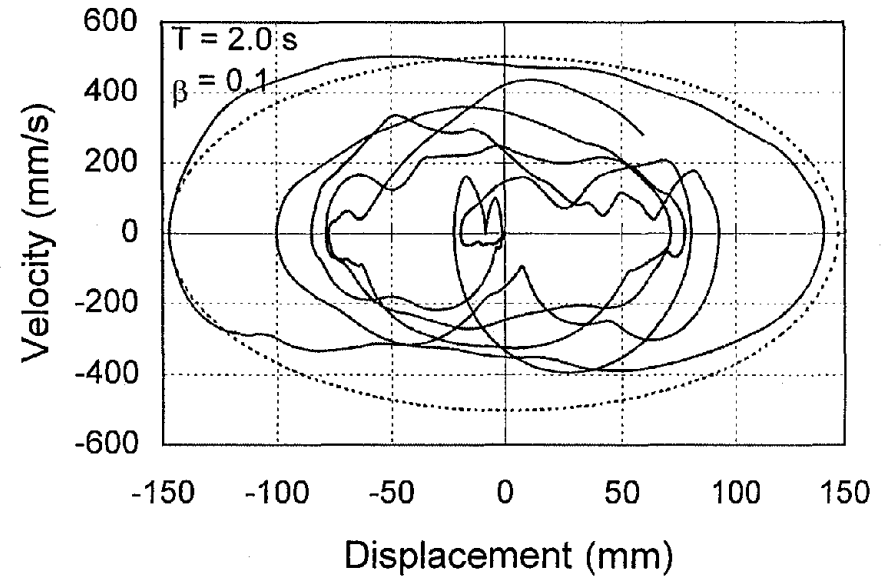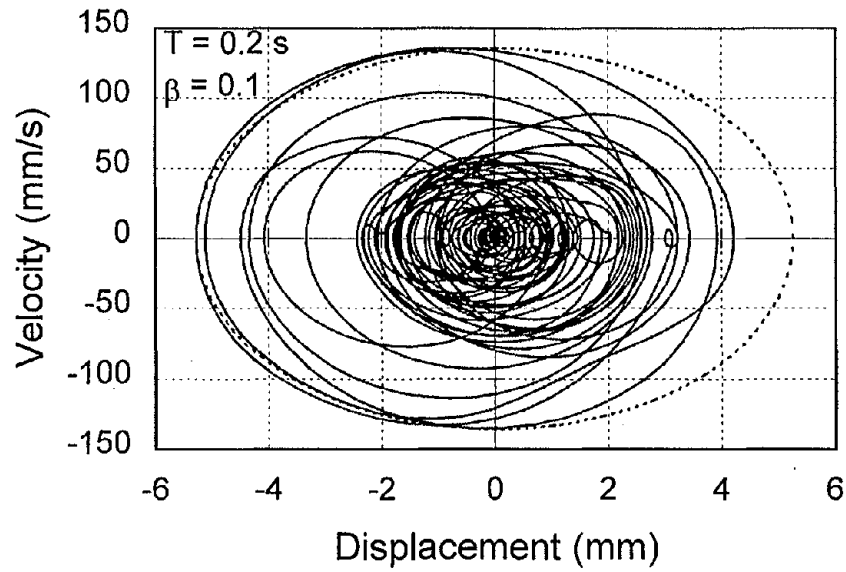$$C_2 = \frac{F_v}{\sqrt{F_d^2 + F_v^2}} \tag{5.5}$$

17

Figure 5.1. Velocity-Displacement Response to the S00E Component of El Centro, Imperial Valley Earthquake, 1940
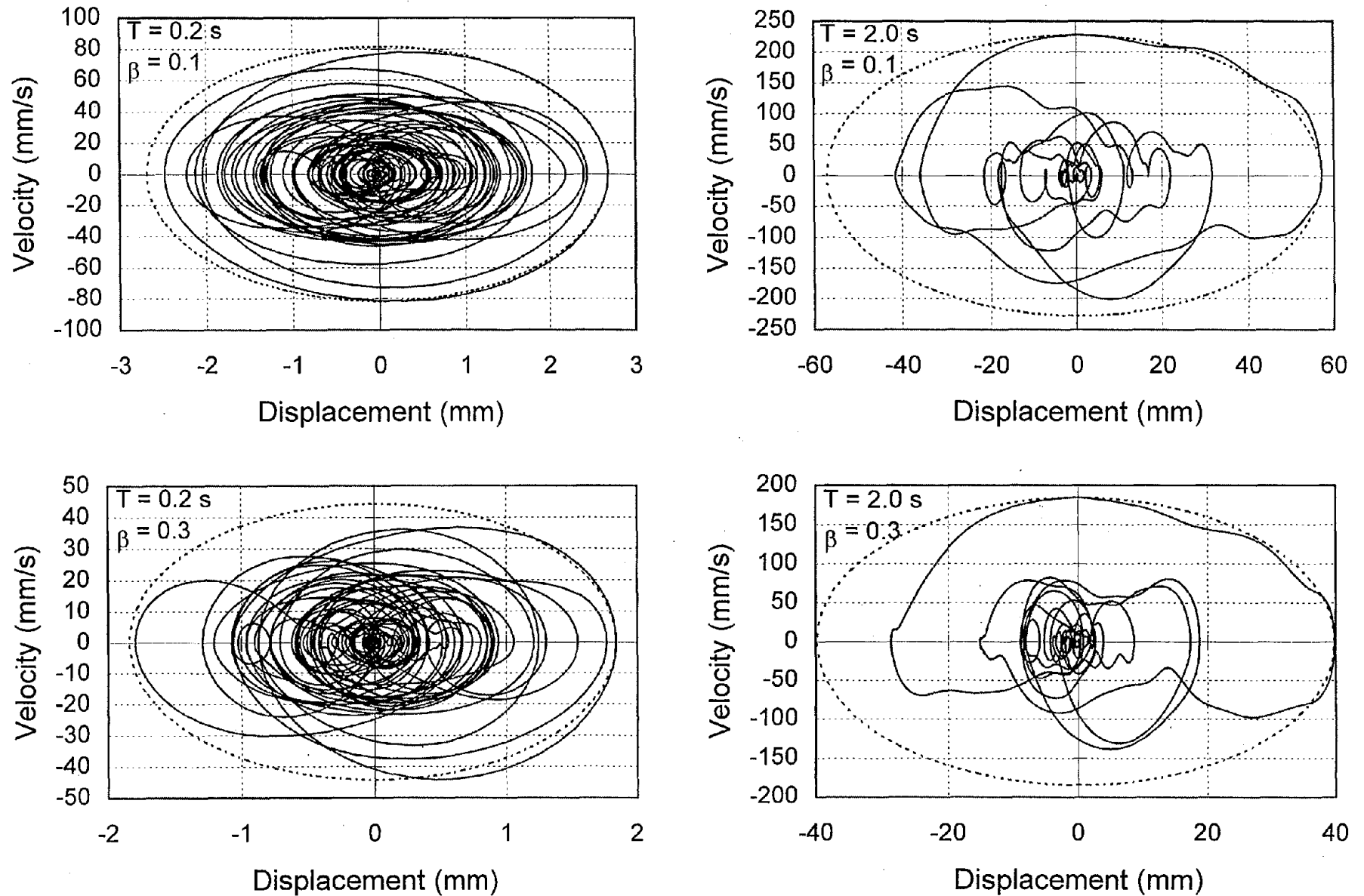
Figure 5.2. Velocity-Displacement Response to the N21E Component of Taft Lincoln School Tunnel, Kern County Earthquake, 1952

Thus, the forces at the stage of maximum acceleration will be computed as the sum of the forces at maximum drift times C_1 and the forces at maximum velocity times C_2. Note that when the force at maximum drift has the same direction as the force at maximum velocity, the peak force at maximum acceleration will be equal to $\sqrt{F_d^2 + F_v^2}$.

To assess the accuracy of the proposed method of computing the design forces, the forces computed from Equations (5.3) to (5.5) were normalized to those for 5 % damping and compared with the mean acceleration ratios from the 72 accelerograms (Figure 4.2). The results of this comparison for damping ratios of 10 %, 20 %, 30 %, 40 %, and 50 % are presented in Figure 5.3. These results show the accuracy of the proposed method. The difference between the force factors computed using the proposed method and those from the average of the 72 ground motion records did not exceed 4 %.

As Equation (5.3) indicates, the design forces will include the contributions of the peak restoring forces and peak damping forces. Figure 5.4 shows the percent contribution of each to the total design forces for damping ratios of 10 %, 20 %, 30 %, 40 %, and 50 %. The figure indicates that, for small damping ratios, at least 90 % of the design forces are due to restoring forces, while for larger damping ratios, the contribution of damping forces is more significant. This is especially true for long-period structures, due to the effect of increased velocities as indicated by Figure 4.3.

5.1   Proposed Linear Static Procedure (LSP)

Based on the above analyses and discussions, the proposed method for the linear static procedure (LSP) can be summarized in the following steps:

1. Compute the fundamental frequency or period of the structure using any of the methods presented in FEMA 273. Assume an effective damping ratio, β_{eff}, in the fundamental mode.
2. Determine the displacement, force, and velocity factors (α_d, α_a, and α_v, respectively) from Tables 5.1 to 5.3 using the computed period and assumed damping ratio.
3. Compute the base shear as the product of the 5 % damped base shear (as given in FEMA 273, Chapter 3) and α_d. Distribute the forces, F_d, along the height of the structure using the method presented in FEMA 273 for conventional structures and compute the design displacements and inter-story drifts.
4. Calculate the effective damping ratio, β_{eff}, using the method outlined in FEMA 273 and iterate on steps 1 through 4 until the desired accuracy is achieved.
5. Compute the velocity between the damper ends as the product of inter-story drift, fundamental frequency, and α_v. Calculate the damper forces as the product of damping coefficient and relative velocity. Estimate the forces acting on the structure at maximum velocity, F_v, due to the damper forces.
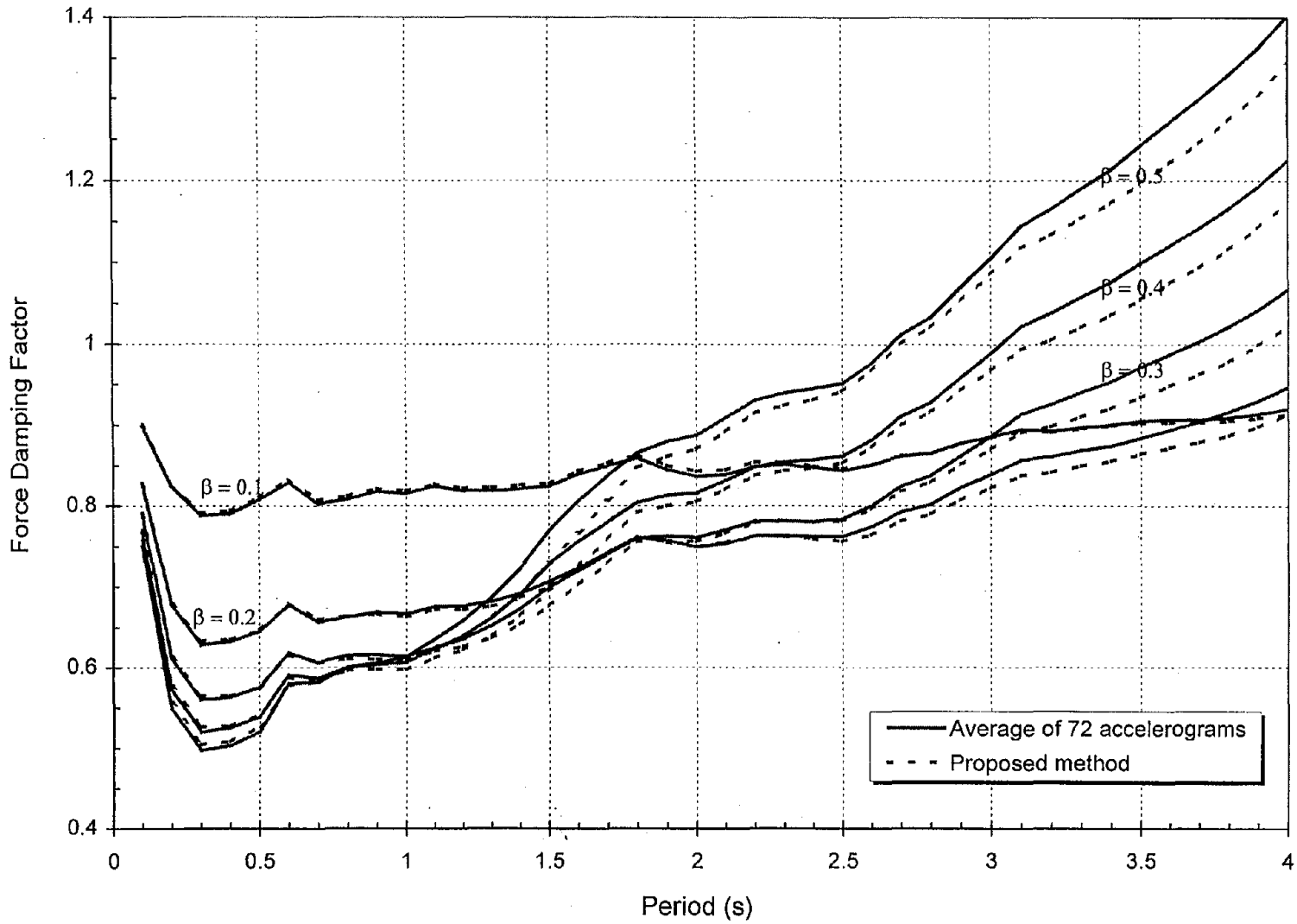
Figure 5.3. Force Damping Factors Using the Proposed Method and Average Time-History Analysis
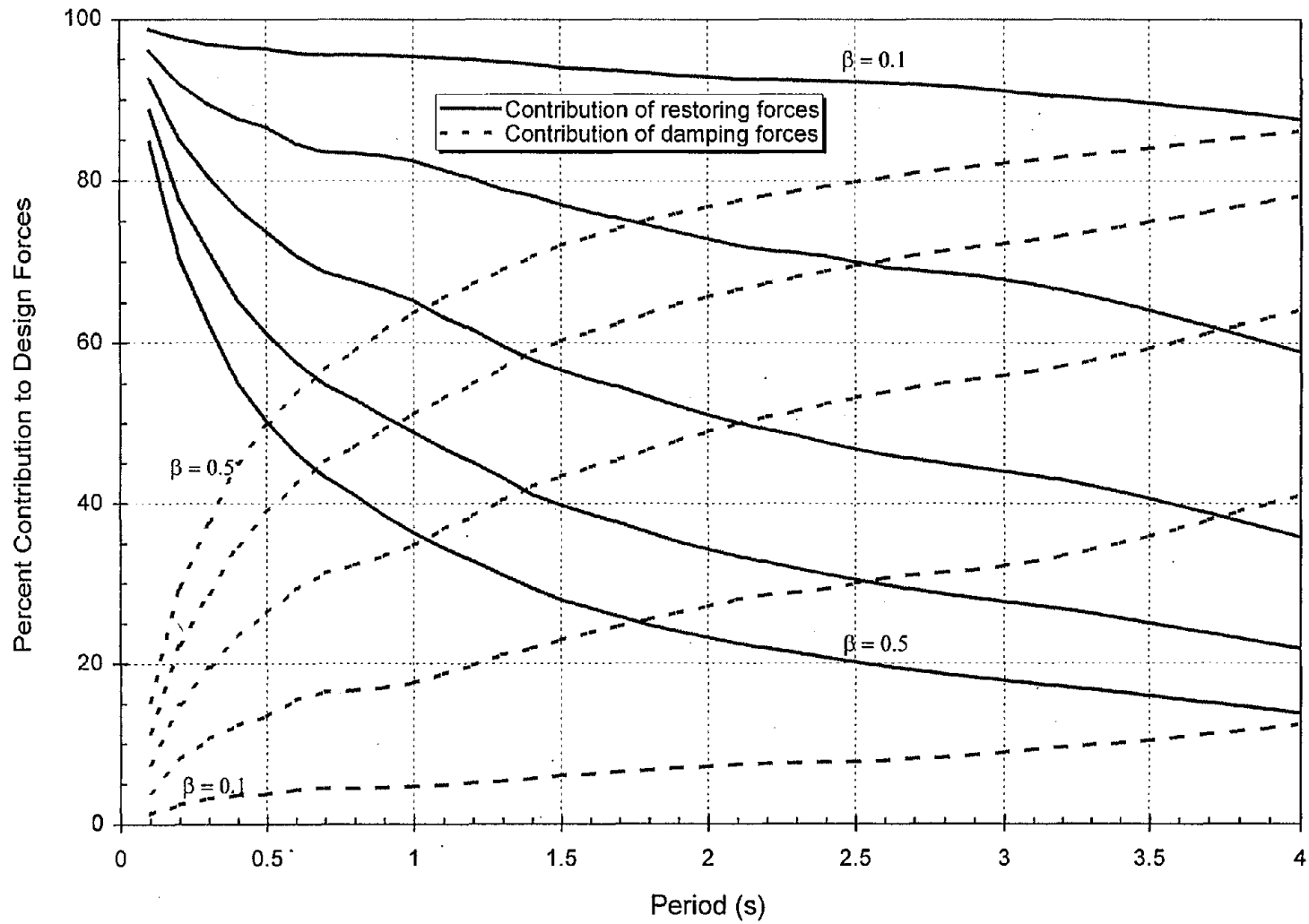
Figure 5.4. Percent Contribution of Restoring and Damping Forces to the Total Design Forces

6. Compute the design forces at the stage of maximum floor acceleration from Equations (5.3) to (5.5). Contrary to FEMA 273 where coefficients CF_1 and CF_2 are the same for all stories, the coefficients C_1 and C_2 will be computed for each story rather than for the whole structure.

7. The final design forces will be selected as the larger of the forces computed at maximum acceleration or at maximum drift (step 3) multiplied by α_a / α_d. This insures that the computed design forces are not less than the 5 % damped forces multiplied by the force factors α_a as recommended in the previous section.

The iterative procedure suggested in step 4 is used since the effective damping ratio, β_{eff}, depends on the displacement in the structures as proposed by FEMA 273. It should be noted that FEMA 273 presents, in addition to the iterative procedure, an expression for estimating β_{eff}. In this formulation, the effective damping ratio is given by:

$$\beta_{eff} = \beta_0 + \frac{T\sum_{j} c_j \cos^2 \theta_j \varphi_{rj}^2}{4\pi \sum_{i} m_i \varphi_i^2} \qquad (5.6)$$

where c_j and θ_j are the damping coefficient and angle of inclination with the horizontal, respectively, of damper j; ϕ_{rj} is the relative modal displacement between the ends of damper j; ϕ_i is the modal displacement of floor i; and m_i is the mass of floor i.

5.2   Proposed Linear Dynamic Procedure (LDP)

A similar procedure to that of the LSP is recommended for the LDP. The procedure, which uses the response spectrum method, is summarized in the following steps:

1. Perform a modal analysis of the structure with the passive energy dissipation devices to compute the natural frequencies and mode shapes. Select the number of modes to be analyzed and assume an effective damping ratio, β_{eff}, in each mode.

2. Determine the displacement, force, and velocity factors (α_d, α_a, and α_v, respectively) from Tables 5.1 to 5.3 for each mode.

3. Multiply the 5 % damped spectral acceleration by α_d for each mode and compute the design displacements, inter-story drifts, and story shears.

4. Calculate the effective damping ratio, β_{eff}, using the method outlined in FEMA 273 and iterate on steps 1 through 4 until the desired accuracy is achieved.

5. Compute the velocity between the damper ends as the product of inter-story drift, frequency, and α_v for each mode. Calculate the damper forces as the product of

23

damping coefficient and relative velocity. Estimate the forces acting on the structure at maximum velocity, F_v, due to the damper forces.

6. Compute the design forces for each mode at the stage of maximum floor acceleration from Equations (5.3) through (5.5). Coefficients C_1 and C_2 should be computed for each story and for each mode.

7. For each mode, the final design forces are selected as the larger of the forces computed at maximum acceleration or at maximum drift (step 3) multiplied by α_a / α_d.

Similar to the LSP, there is no need to perform the iterative procedure in step 4 when Equation (5.6) is used to compute the effective damping ratio. One should combine the modal displacements, velocities, and forces using an appropriate method such as the square root of the sum of squares (SRSS) or the complete quadrature combination (CQC).

6. EXAMPLES AND COMPARISONS

The analysis procedure proposed in this study is compared with that presented in FEMA 273 using several SDOF and MDOF structures. Both procedures are compared with the average results of time history analyses using the 72 accelerograms to assess their accuracy and reliability.

6.1 SDOF Structures

The three key parameters in the design of a structure with supplemental dampers are the design displacement, design velocity, and design force. For a SDOF structure with period T, effective weight W, and no supplemental damping, the design base shear is given as (FEMA 273):

$$V_{uncontrolled} = C_1 C_2 C_3 S_a W = aW \qquad (6.1)$$

where $a = C_1 C_2 C_3 S_a$; S_a is the response spectrum acceleration at the effective fundamental period and damping ratio; and C_1, C_2, and C_3 are modification factors that account for the relationship between peak inelastic and elastic displacements, the effect of stiffness degradation and strength deterioration, and the influence of dynamic second-order effects, respectively (see Section 3.3.1.3 of FEMA 273). Table 6.1 shows the details of the derivations of the three design parameters using the method presented in FEMA 273 and those suggested in this study.

Figures 6.1 to 6.3 present comparisons between the methods proposed herein and in FEMA 273 for the design displacement, velocity, and base shear, respectively, for effective damping ratios of 10 %, 20 %, and 30 %. The figures also show the average results from the time-history analyses. The three figures show the discrepancy between the two design methods (FEMA 273 and this study), especially for larger damping ratios, and indicate the accuracy of the proposed method compared to that in FEMA 273.

Figure 6.1 shows that the two methods give displacements close to each other for periods greater than 0.5 s. For periods shorter than 0.5 s, however, the method presented in FEMA 273 significantly underestimates the displacements. Figure 6.2 shows that the two methods yield velocities close to each other for periods less than 1.0 s. For periods longer than 1.0 s, the FEMA 273 method gives non-conservative velocities and consequently, non-conservative damper forces. Figure 6.3 shows that the method presented in FEMA 273 gives erroneous design forces and it does not capture the increase in design forces for structures with long-periods and large damping ratios.

25

Table 6.1. Design Parameters for SDOF Structures with Supplemental Dampers Using FEMA 273 and Proposed Procedures

Row No.	Design Parameter	FEMA 273		This Study	
		Formulation	Final Equation	Formulation	Final Equation
(1)	Force at max. drift, F_d		$\dfrac{aW}{B}$		$\alpha_d\, aW$
(2)	**Displacement**	$\dfrac{F_d}{k} = \dfrac{F_d}{\left(\dfrac{2\pi}{T}\right)^2 \dfrac{W}{g}}$	$\dfrac{agT^2}{4\pi^2 B}$	$\dfrac{F_d}{k} = \dfrac{F_d}{\left(\dfrac{2\pi}{T}\right)^2 \dfrac{W}{g}}$	$\alpha_d\, \dfrac{agT^2}{4\pi^2}$
(3)	**Velocity**	Displacement $\times \dfrac{2\pi}{T}$	$\dfrac{agT}{2\pi B}$	Displacement $\times\ \alpha_v\ \times \dfrac{2\pi}{T}$	$\alpha_v \alpha_d\, \dfrac{agT}{2\pi}$
(4)	Force at max. velocity, F_v	$c \times$ velocity $=$ $2\dfrac{W}{g}\dfrac{2\pi}{T}\beta \times$ velocity	$2\beta\dfrac{aW}{B}$	$c \times$ velocity $=$ $2\dfrac{W}{g}\dfrac{2\pi}{T}\beta \times$ velocity	$2\beta\alpha_d\alpha_v aW$
(5)	Force at max. acceleration	$CF_1 F_d + CF_2 F_v$	$\dfrac{aW}{B}(CF_1 + 2\beta CF_2)$	$C_1 F_d + C_2 F_v$	$\alpha_d\, aW\sqrt{1+(2\beta\alpha_v)^2}$
(6)	**Final base Shear**	largest of **(1)**, **(4)**, and **(5)**	$\dfrac{aW}{B}(CF_1 + 2\beta CF_2)$	larger of **(5)** and $F_d\dfrac{\alpha_a}{\alpha_d}$	$\alpha_a aW$

Figure 6.1. Design Displacement for SDOF Structures Using Time-History, and the Methods Proposed in this Study and in FEMA 273

The figure shows a plot with:
- Y-axis: Velocity x $(2\pi / agT)$, ranging from 0.2 to 1.6
- X-axis: Period (s), ranging from 0 to 4
- Legend annotations: $= 0.1$ top, $\beta = 0.2$, $= 0.3$ bottom
- Legend: Time History, This Study, FEMA 273

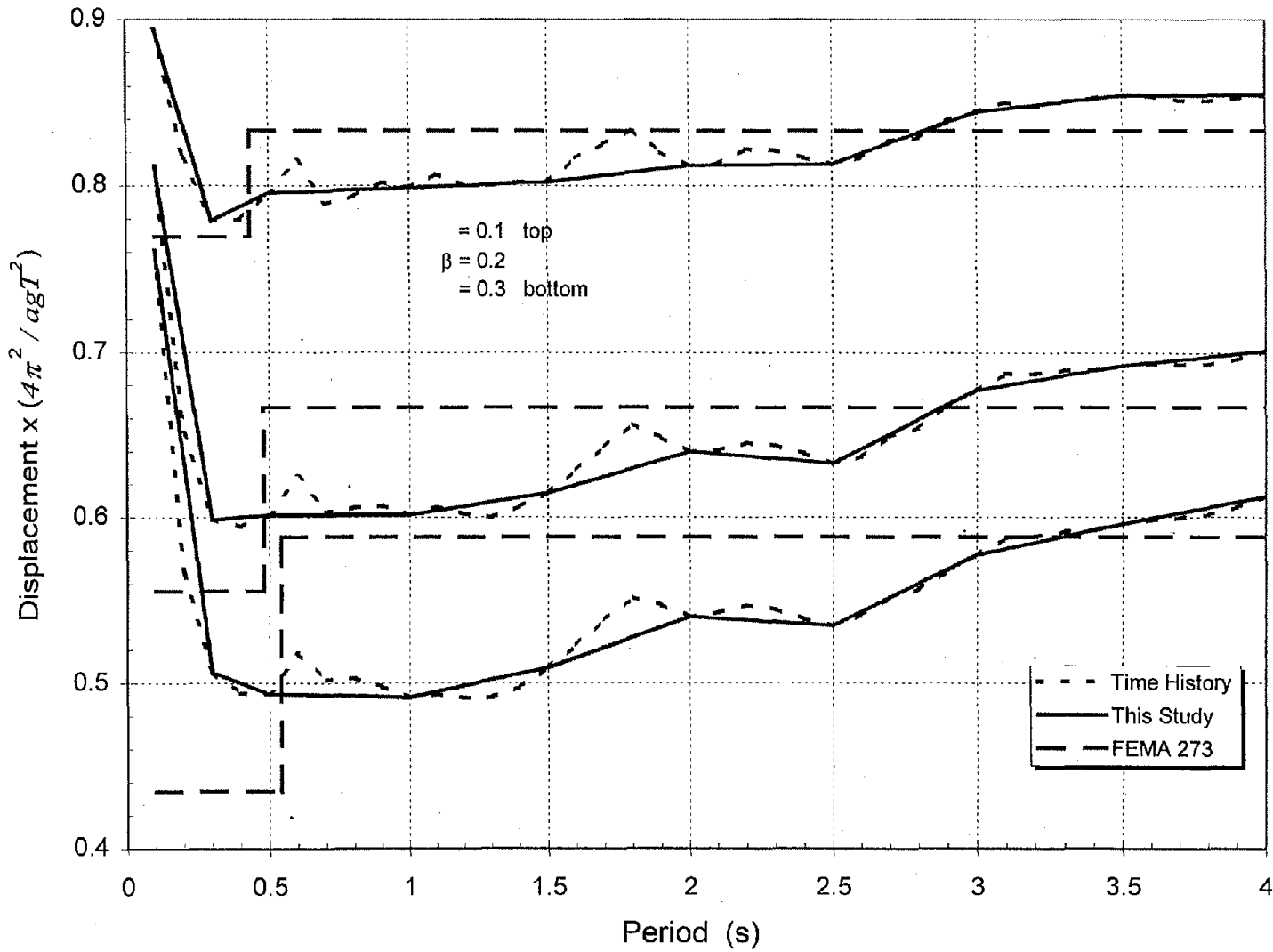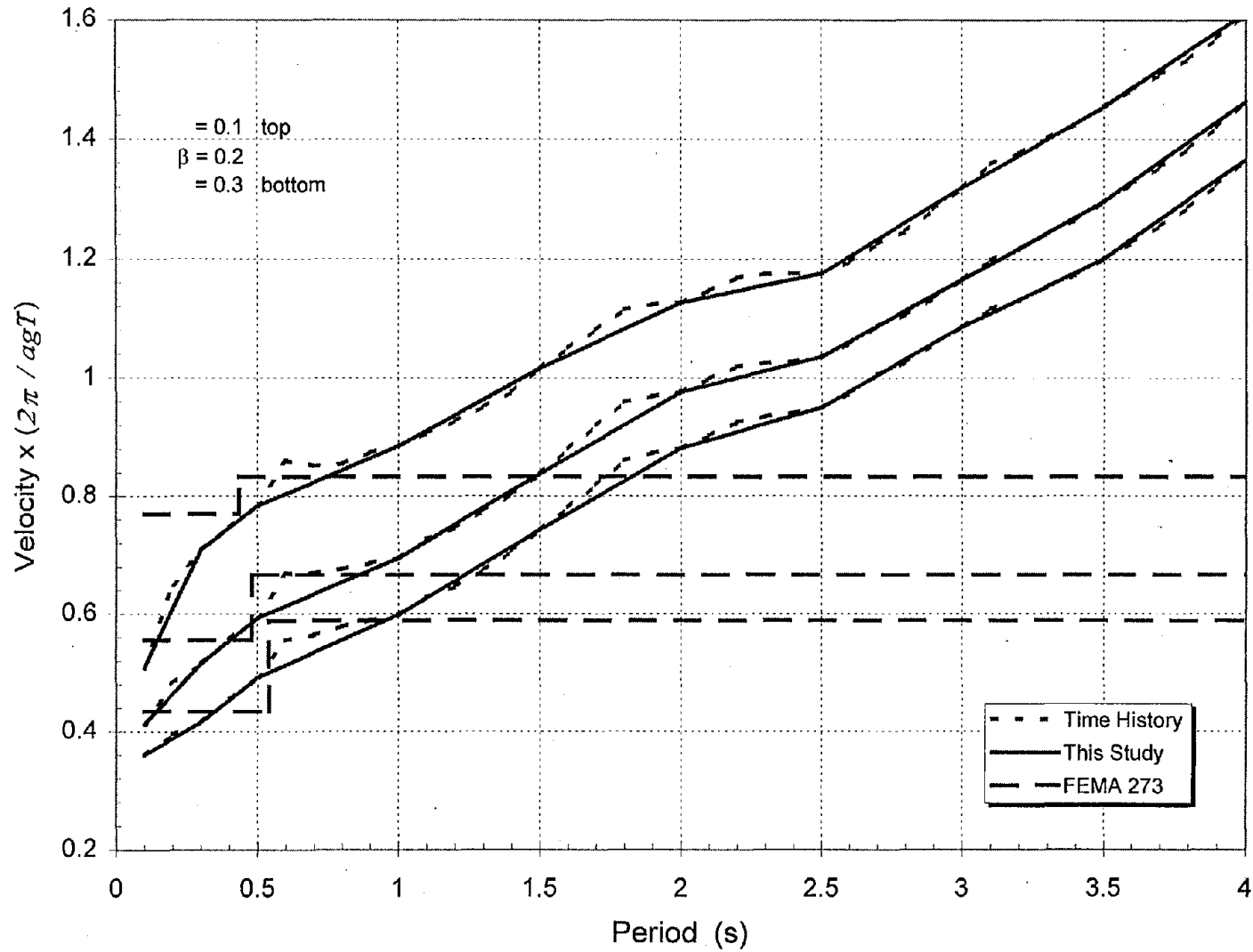Figure 6.2. Design Velocity of SDOF Structures Using Time-History, and the Methods Proposed in this Study and in FEMA 273
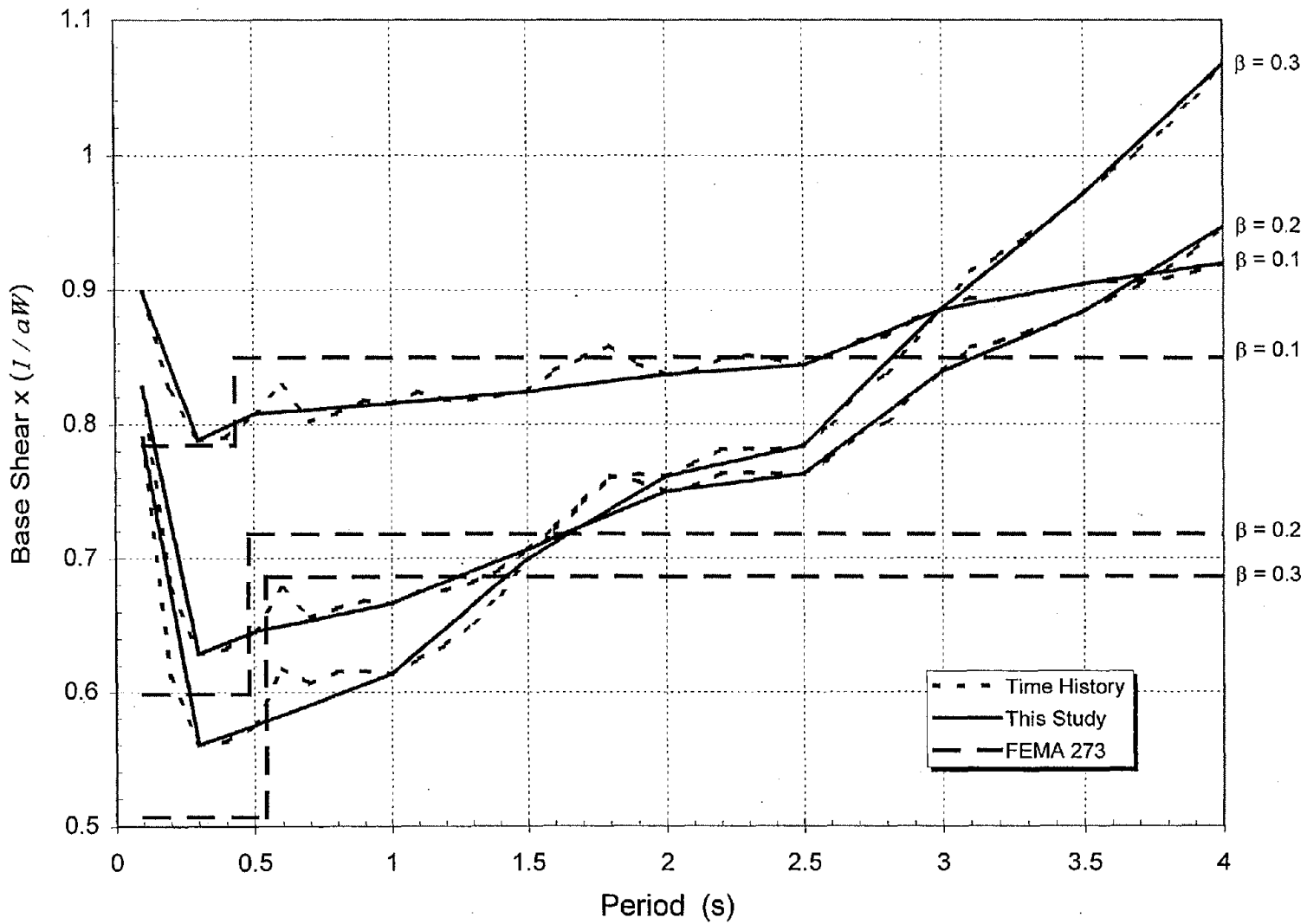
Figure 6.3. Design Base Shear for SDOF Structures Using Time-History, and the Methods Proposed in this Study and in FEMA 273
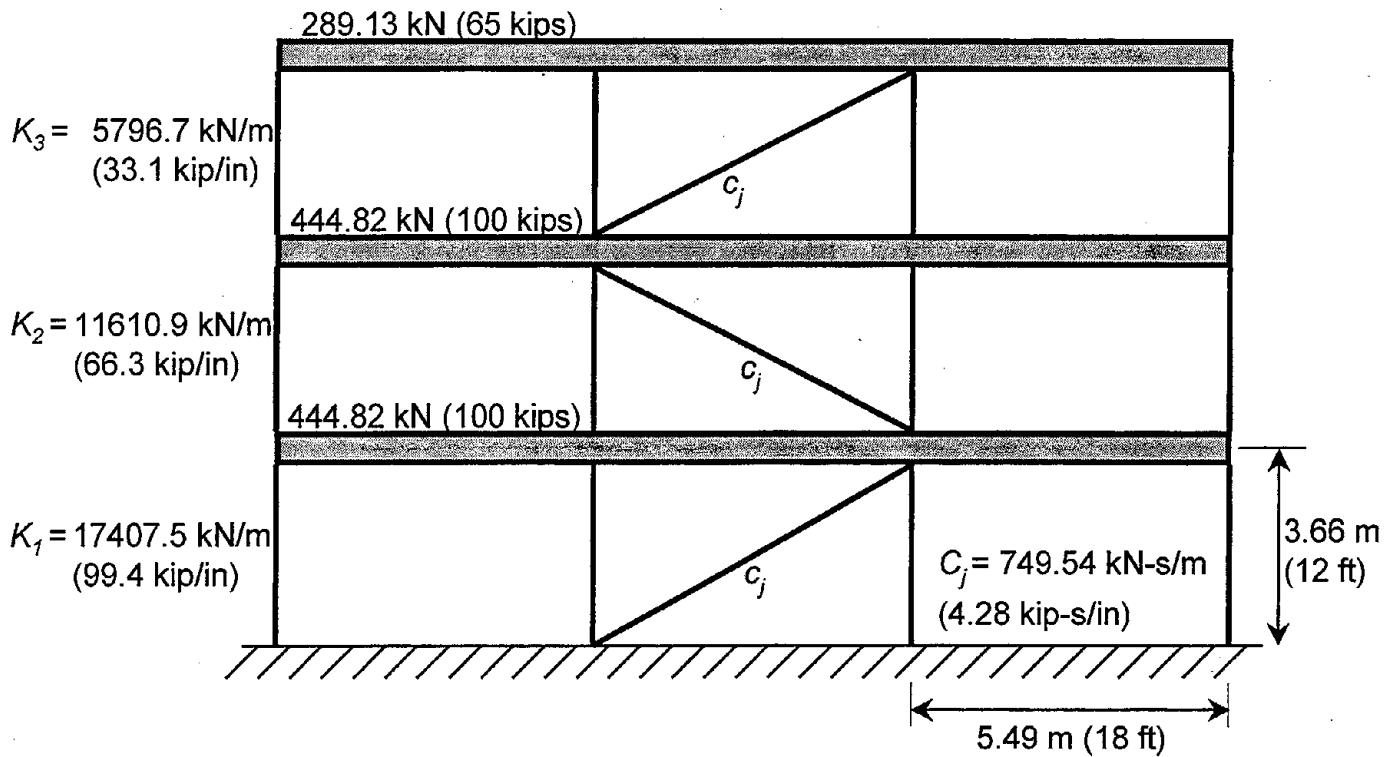
6.2 MDOF Structures

The commentary on FEMA 273 (FEMA 274) includes a design example of a three-story building with supplemental viscous dampers in every story. The same example is used in this study and the results are compared with those from FEMA 273. The building properties are shown in Figure 6.4. The building has a fundamental period of 0.75 s and an inherent damping ratio of 0.05. The damping coefficient of the dampers was adjusted to result in a damping ratio of 0.25 in the fundamental mode.

Table 6.2 shows the details of the LSP suggested in this study and that in FEMA 273. Similarly, Table 6.3 shows the results using the LDP for both methods. The tables show significant differences between the methods recommended by FEMA 273 and those proposed in this study (approximately 11 % in displacements, 21 % in velocities and damper forces, and 28 % in shear forces). To investigate the accuracy of the two methods, the same structure, with and without dampers, was analyzed using the 72 earthquake records. Figure 6.5 shows the floor displacements normalized to the uncontrolled roof displacement, the floor velocities normalized to the uncontrolled roof velocity, and the story shears normalized to the uncontrolled base shear. The plots in Figure 6.5 are presented for the structure with and without supplemental dampers using the LSPs recommended in this study and in FEMA 273 as well as the average from the time history analyses. The accuracy of the proposed method can be seen through a comparison with the results of the time history analysis. Results using the LDP (not presented) also showed similar trends to those in Figure 6.5.

To investigate the accuracy of the proposed method for other structural periods, the frame was re-analyzed twice. In the second analysis, the weight of all floors was set equal to 75.62 kN (17 kips) and the column stiffnesses were multiplied by 3 which resulted in a fundamental period of 0.2 s. For this case, the damping coefficient of the supplemental dampers was selected as 554.10 kN-s/m (3.164 kip-s/in) to achieve an equivalent damping ratio of 0.25 in the fundamental mode using Equation (5.6). The structure with and without supplemental dampers was analyzed using both the LSPs suggested in this study and in FEMA 273 in addition to time history analyses using the 72 accelerograms. Plots of the normalized peak responses are presented in Figure 6.6 for this structure. The plot for the displacement response shows the accuracy of the proposed method as compared to that recommended by FEMA 273. The design displacements and forces from this study are much closer to those from the time history analysis than those using the FEMA 273 procedure.

In the third analysis, the weight of all floors was set equal to 2402.03 kN (540 kips) and the column stiffnesses were kept the same as the original structure. This resulted in a fundamental period of 2.0 s. For this case, the damping coefficient of the supplemental dampers was selected as 1802.7 kN-s/m (10.294 kip-s/in) to achieve an equivalent damping ratio of 0.25 in the fundamental mode using Equation (5.6). This structure was analyzed using the same procedures as before and plots of the normalized peak responses are presented in Figure 6.7. The plots indicate significant differences between the results using the LSP from this study, FEMA 273, and the time history analysis. The reasons for such differences are: 1) the distribution of the lateral forces for the structure without supplemental dampers as recommended by FEMA 273 is significantly different from the actual distribution using time

30

289.13 kN (65 kips)

$K_3 =$ 5796.7 kN/m
(33.1 kip/in)

444.82 kN (100 kips)

c_j

$K_2 =$ 11610.9 kN/m
(66.3 kip/in)

444.82 kN (100 kips)

c_j

$K_1 =$ 17407.5 kN/m
(99.4 kip/in)

c_j

$C_j =$ 749.54 kN-s/m
(4.28 kip-s/in)

3.66 m
(12 ft)

5.49 m (18 ft)

Modal Properties

		Mode 1	Mode 2	Mode 3
Period (s)		0.75	0.34	0.22
Frequency (rad/s)		8.38	18.45	28.46
Mode Shape	roof	1.00	1.00	1.00
	2	0.64	-0.73	-3.10
	1	0.29	-0.62	4.67
Modal Participation Factor		1.38	0.45	0.07
Effective Damping Ratio		0.25	0.67	0.63

Figure 6.4. Properties of the three-story building

31

Table 6.2. Analysis of the Three-Story Building Using the LSP

Fundamental period T = 0.75 s		Effective damping ratio = 0.25
α_d = 0.545 (Table 3)	α_v = 1.089 (Table 5)	α_a = 0.625 (Table 4)

Story (1)	lateral load at max. drift, F_d kN (kips) (2)	story shear at max. drift kN (kips) (3)	floor displacement m (in) (4)	floor velocity m/s (in/s) (5)	inter-story drift m (in) (6)	inter-story velocity m/s (in/s) (7)	damper axial force kN (kips) (8)
	α_d × 5% damped forces	from (2)	structural analysis	$\omega \times \alpha_v \times$ (4)	from (4)	from (5)	$c \times \cos\theta \times$ (7)
roof	263.3 (59.2)	263.3 (59.2)	0.127 (5.006)	1.160 (45.684)	0.045 (1.789)	0.415 (16.326)	258.6 (58.13)
2	257.1 (57.8)	520.4 (117.0)	0.082 (3.217)	0.746 (29.358)	0.045 (1.764)	0.409 (16.098)	255.0 (57.32)
1	121.9 (27.4)	642.3 (144.4)	0.037 (1.453)	0.337 (13.260)	0.037 (1.453)	0.337 (13.260)	210.0 (47.22)

Story (1)	lateral load at max. velocity, F_v kN (kips) (9)	C_1 and C_2 (10)	lateral load at max. acceleration kN (kips) (11)	story shear at max. acceleration kN (kips) (12)	$\alpha_a / \alpha_d \times$ story shear at max. drift kN (kips) (13)	final story shear kN (kips) (14)
	from (8)	Equations 14 and 15 and from (2) and (9)	$C_1 \times$ (2) + $C_2 \times$ (9)	from (11)	$\alpha_a / \alpha_d \times$ (3)	Larger of (12) and (13)
roof	215.3 (48.4)	0.7742 0.6330	339.8 (76.4)	339.8 (76.4)	302.0 (67.9)	339.8 (76.4)
2	-3.1 (-0.7)	0.9999 0.0121	257.1 (57.8)	596.9 (134.2)	596.9 (134.2)	596.9 (134.2)
1	-37.4 (-8.4)	0.9561 0.2931	105.4 (23.7)	702.3 (157.9)	736.6 (165.6)	702.3 (165.6)

Story (1)	FEMA 273			
	floor displacement m (in) (15)	floor velocity m/s (in/s) (16)	damper axial force kN (kips) (17)	final story shear kN (kips) (18)
roof	0.114 (4.504)	0.959 (37.744)	214.0 (48.1)	291.8 (65.6)
2	0.073 (2.891)	0.615 (24.226)	210.8 (47.4)	497.3 (111.8)
1	0.033 (1.301)	0.277 (10.902)	172.6 (38.8)	578.3 (130.0)

Table 6.3. Analysis of the Three-Story Building Using the LDP

Row No.	Response quantity	Formulation	level	Mode 1	Mode 2	Mode 3	SRSS	FEMA 273
(1)	α_d α_v α_a	Table 3 Table 5 Table 4		0.545 1.089 0.625	0.356 0.814 0.486	0.484 0.624 0.584		
(2)	uncontrolled spectral acceleration (g)			1.0	1.0	1.0		
(3)	damped spectral displacement m (in)	$(\alpha_d)_i \times (2)/\omega_i^2$		0.076 (3.000)	0.010 (0.402)	0.006 (0.231)		
(4)	floor displacement m (in)	(mode shape)$_i$ × (participation factor)$_i$ × (3)	3 2 1	0.105 (4.14) 0.067 (2.65) 0.030 (1.20)	0.005 (0.18) -0.003 (-0.13) -0.003 (-0.11)	0.001 (0.02) -0.001 (-0.05) 0.002 (0.08)	0.105 (4.14) 0.067 (2.65) 0.031 (1.21)	0.094 (3.70) 0.061 (2.39) 0.027 (1.08)
(5)	lateral load at max. drift, F_d kN (kips)	analysis	3 2 1	219.3 (49.3) 208.2 (46.8) 102.8 (23.1)	45.8 (10.3) -51.6 (-11.6) -44.0 (-9.9)	9.8 (2.2) -46.7 (-10.5) 70.3 (15.8)		
(6)	story shear at max drift kN (kips)	from (5)	3 2 1	219.3 (49.3) 427.5 (96.1) 530.3 (119.2)	45.8 (10.3) 5.8 (1.3) 49.8 (11.2)	9.8 (2.2) 36.9 (8.3) 33.4 (7.5)		
(7)	floor velocity m/s (in/s)	$(\alpha_v)_i \times \omega_i \times (4)$	3 2 1	0.960 (37.78) 0.614 (24.18) 0.278 (10.95)	0.069 (2.70) -0.050 (-1.95) -0.042 (-1.65)	0.007 (0.28) -0.023 (-0.89) 0.045 (1.33)	0.962 (37.88) 0.616 (24.27) 0.283 (11.15)	0.791 (31.16) 0.510 (20.08) 0.237 (9.31)
(8)	inter-story drift m (in)	from (4)	3 2 1	0.038 (1.49) 0.037 (1.45) 0.030 (1.20)	0.008 (0.31) 0.001 (0.02) 0.003 (0.11)	0.002 (0.07) 0.003 (0.13) 0.002 (0.08)	0.039 (1.52) 0.037 (1.46) 0.031 (1.21)	0.034 (1.34) 0.034 (1.32) 0.027 (1.08)
(9)	inter-story velocity m/s (in/s)	from (7)	3 2 1	0.345 (13.60) 0.336 (13.23) 0.278 (10.95)	0.118 (4.65) 0.008 (0.30) 0.042 (1.65)	0.030 (1.17) 0.056 (2.22) 0.045 (1.33)	0.366 (14.42) 0.341 (13.42) 0.283 (11.15)	0.313 (12.34) 0.284 (11.20) 0.237 (9.31)

33

Table 6.3. Continued

| Row No.	Response quantity	Formulation	level	Mode 1	Mode 2	Mode 3	SRSS	FEMA 273
(10)	damper axial force kN (kips)	$c_0 \times \cos\theta \times$ (9)	3	215.3 (48.4)	73.8 (16.6)	18.7 (4.2)	228.6 (51.4)	195.7 (44.0)
			2	209.5 (47.1)	4.9 (1.1)	35.6 (8.0)	212.6 (47.8)	178.8 (40.2)
			1	173.5 (39.0)	26.2 (5.9)	21.4 (4.8)	177.0 (39.8)	147.2 (33.1)
(11)	lateral load at max. velocity, F_v kN (kips)	from (10)	3	179.3 (40.3)	61.4 (13.8)	15.6 (3.5)		
			2	-4.9 (-1.1)	-65.4 (-14.7)	-45.4 (-10.2)		
			1	-29.8 (-6.7)	-17.8 (-4.0)	47.6 (10.7)		
(12)	C_1 and C_2	Equations 14 and 15 and from (5) and (11)	3	0.77 0.63	0.60 0.80	0.53 0.85		
			2	0.99 0.02	0.62 0.78	0.72 0.70		
			1	0.96 0.28	0.93 0.37	0.83 0.56		
(13)	lateral load at max. acceleration kN (kips)	$C_1 \times$ (5) + $C_2 \times$ (11)	3	283.4 (63.7)	86.7 (19.5)	18.2 (4.1)		
			2	207.7 (46.7)	-83.2 (-18.7)	-64.9 (-14.6)		
			1	90.3 (20.3)	-47.6 (-10.7)	85.0 (19.1)		
(14)	story shear at max. acceleration kN (kips)	from (13)	3	283.4 (63.7)	86.7 (19.5)	18.2 (4.1)		
			2	491.1 (110.4)	3.5 (0.8)	46.7 (10.5)		
			1	581.4 (130.7)	44.1 (9.9)	38.3 (8.6)		
(15)	story shear at max drift $\times\ \alpha_a / \alpha_d$ kN (kips)	$\alpha_a / \alpha_d \times$ (6)	3	251.3 (56.5)	62.7 (14.1)	12.0 (2.7)		
			2	490.2 (110.2)	8.0 (1.8)	44.5 (10.0)		
			1	608.1 (136.7)	68.1 (15.3)	40.0 (9.0)		
(16)	final story shear kN (kips)	Larger of (14) and (15)	3	283.4 (63.7)	86.7 (19.5)	18.2 (4.1)	296.7 (66.7)	253.1 (56.9)
			2	491.1 (110.4)	8.0 (1.8)	46.7 (10.5)	493.3 (110.9)	411.5 (92.5)
			1	608.1 (136.7)	68.1 (15.3)	40.0 (9.0)	613.0 (137.8)	477.7 (107.4)
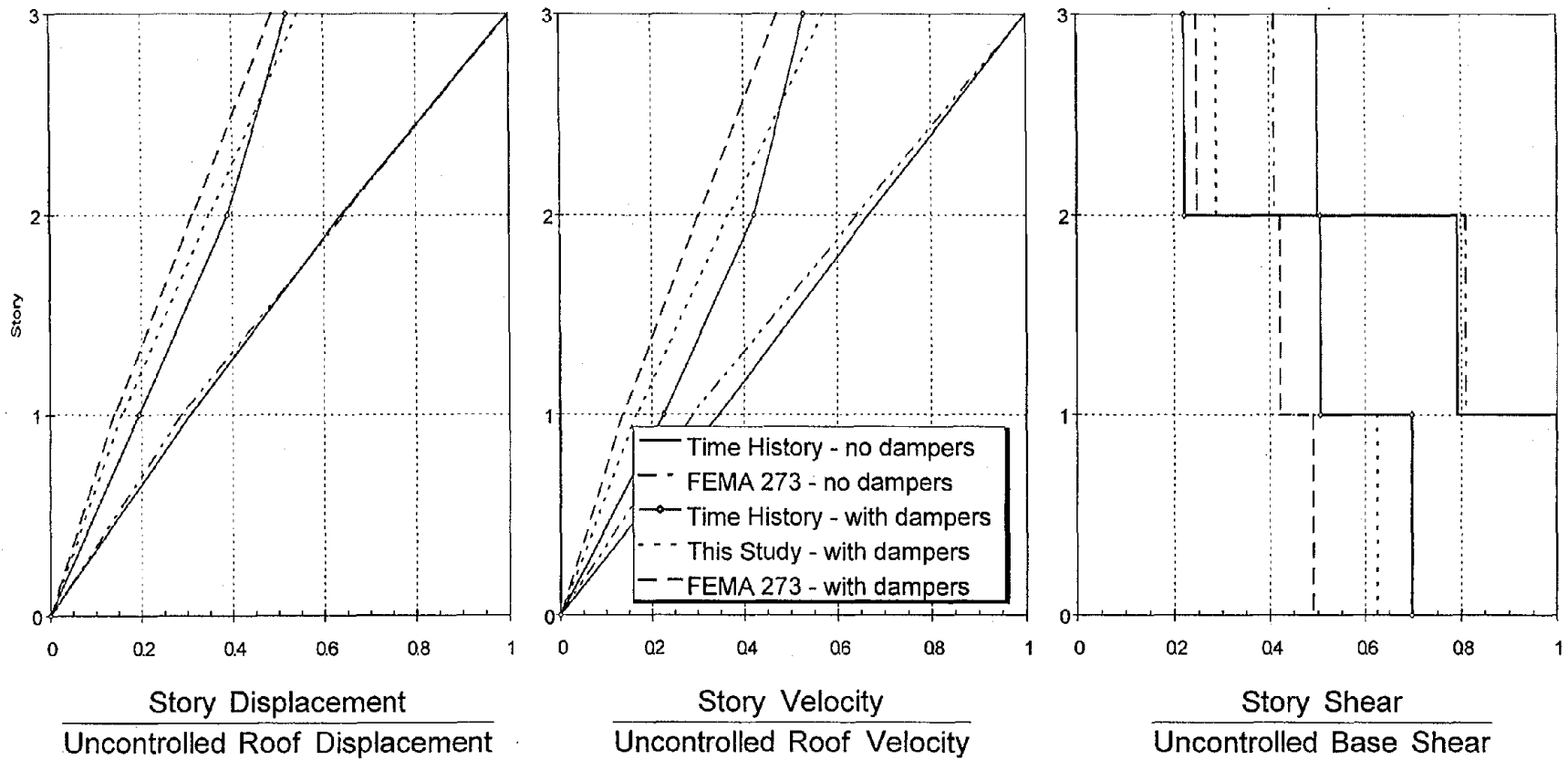
Figure 6.5. Peak Response of the Three-Story Building (T = 0.75 s) with and without Supplemental Dampers
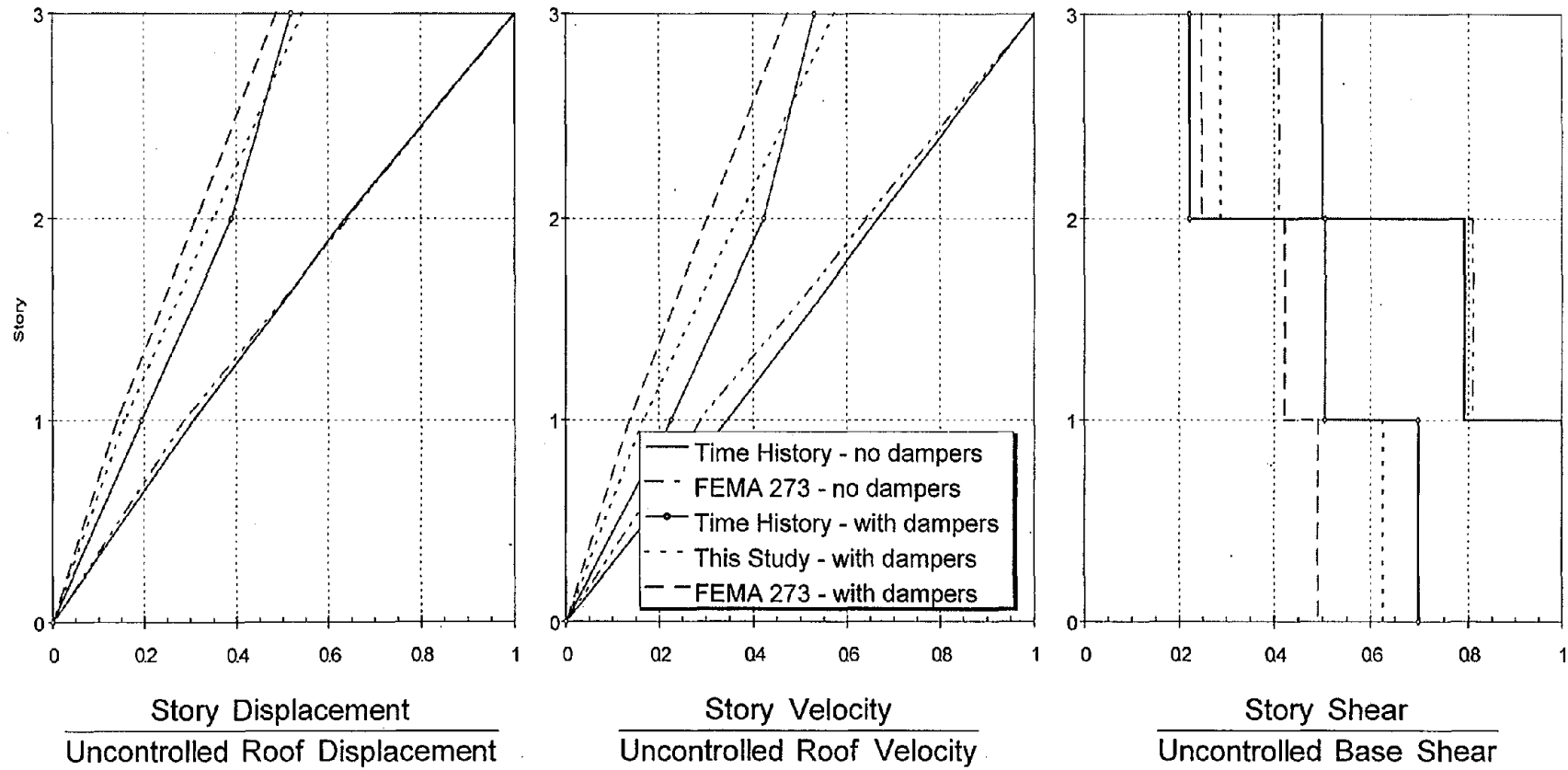
Figure 6.6. Peak Response of the Three-Story Building (T = 0.20 s) with and without Supplemental Dampers

Legend
Time History - no dampers
FEMA 273 - no dampers
Time History - with dampers
This Study - with dampers
FEMA 273 - with dampers

Story Displacement / Uncontrolled Roof Displacement

Story Velocity / Uncontrolled Roof Velocity
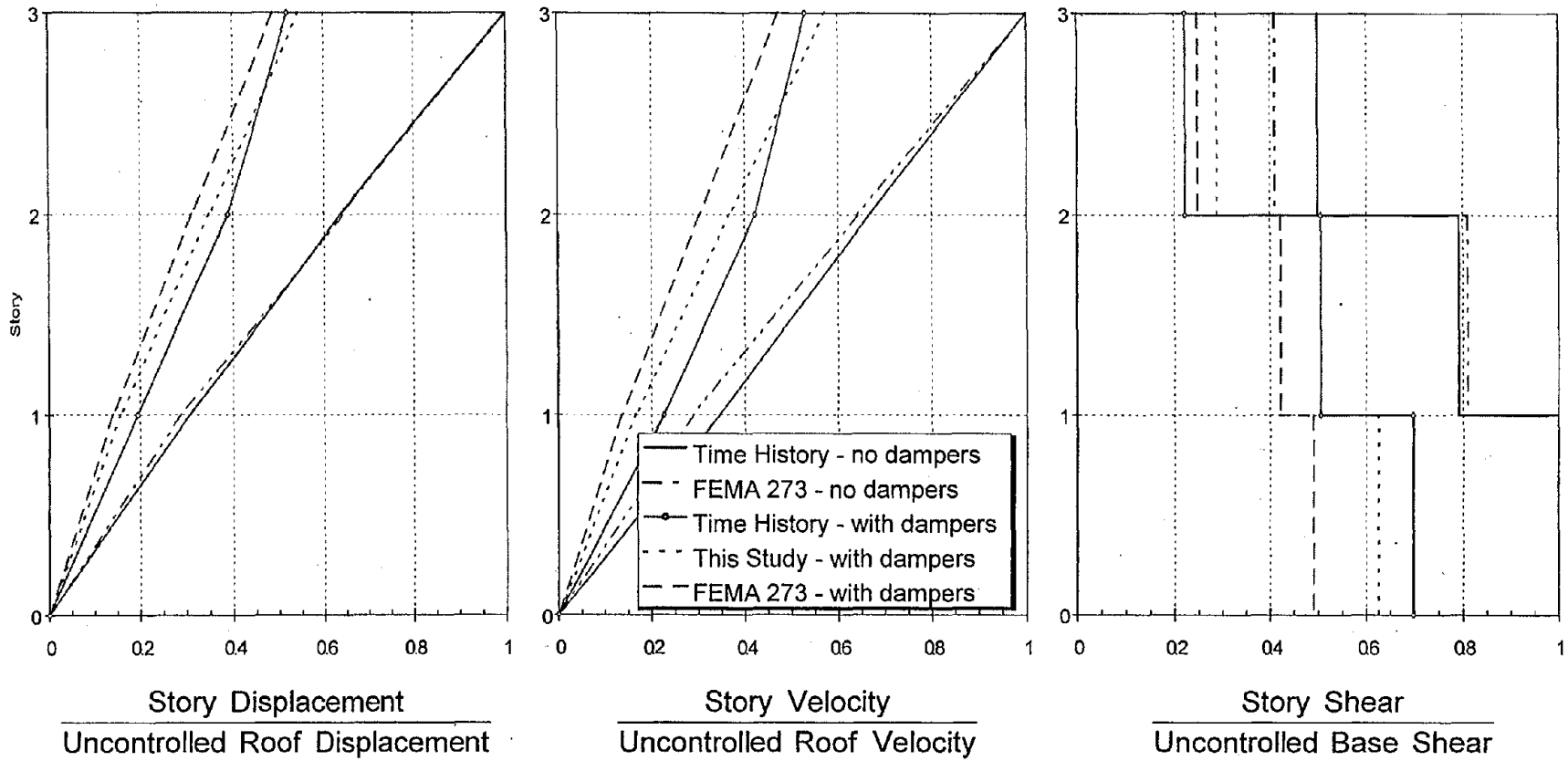
Story Shear / Uncontrolled Base Shear

Figure 6.7. Peak Response of the Three-Story Building (T = 2.0 s) with and without Supplemental Dampers

history analysis, as seen in Figure 6.7; 2) the contribution of higher modes for long-period structures, which is not accounted for in the LSP; and 3) the difference between the response using discrete dampers in the time history analysis and the approximation of using an equivalent damping ratio in the LSP. It should be noted, however, that generally, the method suggested in this study resulted in a closer response to the time history analysis than the FEMA 273 method, especially for the base shear.

7. CONCLUSIONS

The overall objectives of this study were: 1) to investigate the effect of increased viscous damping on the seismic response of structures, 2) to assess the accuracy of the linear static (LSP) and linear dynamic (LDP) procedures recommended by FEMA 273 for designing structures with velocity-dependent passive energy dissipation devices, and 3) to propose modifications to the current design procedures to achieve better accuracy and reliability. The findings of the study, based on the analysis of several SDOF and MDOF structures using an ensemble of 72 earthquake records, can be summarized as follows:

1. Increasing damping in structures allows more input seismic energy to be dissipated, which generally reduces the response of structures. The reduction, however, depends on the structural period and the amount of supplemental damping. For example, the effect of damping on the displacement response is more pronounced in the velocity region (structures with periods in the range of 0.3 s to 0.5 s). For long-period structures, an increase in damping further decreases the displacement response, but increases the absolute acceleration response and consequently seismic forces.

2. Design forces should include the contributions of the peak restoring forces and peak damping forces. The study indicates that for small damping ratios, approximately 90 % of the design forces are due to the restoring forces, while for larger damping ratios, the contribution of damping forces is more significant. This is especially true for long-period structures, due to the effect of increased velocities.

3. The LSP and LDP recommended by FEMA 273 have the following limitations: a) they use a constant reduction factor for the displacement response in the acceleration region of the spectrum. This assumption can result in a non-conservative design in short-period structures, b) they assume a harmonic response to compute the peak velocity, i.e., the peak velocity is equal to the pseudo-velocity. This assumption results in accurate velocities, and consequently damper forces, only for structures with periods close to 0.5 s. This study, however, shows that for structures with other periods, the pseudo-velocity should be multiplied by a factor that depends on the structural period and the damping ratio, and c) they assume that the structure undergoes a harmonic motion with an amplitude equal to the peak displacement and a frequency equal to that of the fundamental (or a given) mode. Consequently, the same coefficients are used in each story to compute the design forces. This study shows that assuming an elliptical peak displacement-velocity response and using different coefficients for each story to compute the design forces is more accurate.

4. Modifications to the LSP and LDP presented in FEMA 273 are recommended in this study based on the analysis of SDOF structures subjected to 72 earthquake records. Comparisons between the method proposed in this study and that in FEMA 273 show that the method presented herein is more accurate when compared with the time-history analysis of three MDOF structures.

39

One of the limitations of the LSP and LDP for design of structures with velocity-dependent energy dissipation devices is that they should be used only for linearly elastic structures. Since structures may undergo nonlinear behavior under severe earthquake excitations and for wider applications of the procedures, additional research is needed to extend the linear procedures to include structures with nonlinear behavior.

REFERENCES

Ashour, S. A., and Hanson, R. D. (1987). "Elastic seismic response of buildings with supplemental damping." *Report UMCE 87-1*, Dept. of Civil Engrg., The University of Michigan, Ann Arbor, Michigan.

Chopra, A. K. (1995). *Dynamics of structures*, Prentice Hall, Englewood Cliffs, New Jersey.

FEMA 273 (1997). "NEHRP guidelines for the seismic rehabilitation of buildings." Building Seismic Safety Council, Washington, D.C.

FEMA 274 (1997). "NEHRP commentary on the guidelines for the seismic rehabilitation of buildings." Building Seismic Safety Council, Washington, D.C.

Hanson, R. D., Aiken, I. D., Nims, D. K., Richter, P. J., and Bachman, R. E. (1993). "State-of-the-art and state-of-the-practice in seismic energy dissipation." *Proc., ATC-17-1 Seminar on Seismic Isolation, Passive Energy Dissipation, and Active Control*, Vol. 2, Applied Technology Council, Redwood City, California, pp. 449-471.

NEHRP 1994 (1995). "NEHRP recommended provisions for seismic regulations for new buildings." FEMA 223, Building Seismic Safety Council, Washington, D.C.

NEHRP 1997 (1998). "NEHRP recommended provisions for seismic regulations for new buildings and other structures." FEMA 302, Building Seismic Safety Council, Washington, D.C.

Newmark, N. M., and Hall, W. J. (1982). "Earthquake spectra and design." *Monograph Series*, Earthquake Engrg. Res. Inst., Oakland, California.

Tsopelas, P., Constantinou, M. C., Kircher, C. A., and Whittaker, A. S. (1997). "Evaluation of simplified methods of analysis for yielding structures," *Technical Report No. NCEER-97-0012*, National Center for Earthquake Engineering Research, Buffalo, New York.

UBC 1994 (1994). Uniform Building Code, International Conference of Building Officials, Whittier, California.

UBC 1997 (1997). Uniform Building Code, International Conference of Building Officials, Whittier, California.

Whittaker, A. S., Constantinou, M. C., and Kircher, C. A. (1996). "Seismic rehabilitation using supplemental damping systems," *Proc., 11th World Conference on Earthquake Engineering*, Acapulco, Mexico, Paper No. 430.

Whittaker, A. S., Constantinou, M. C., and Kircher, C. A. (1997). "Analysis of buildings incorporating supplemental dampers," *Proc., The EERC-CUREe Symposium in Honor of Vitelmo V. Bertero*, Berkeley, California, pp. 141-148.

Wu, J., and Hanson, R. D. (1989). "Study of inelastic spectra with high damping." *J. Struct. Engrg.*, ASCE, Vol. 115(6), pp. 1412-1431.

APPENDIX A. EARTHQUAKE RECORDS USED IN THE STATISTICAL STUDY

Earthquake	Mag.	Station Name	Source Distance (km)	Comp.	Peak Accel. (g)
Imperial Valley 05/18/1940	6.7	El Centro Valley Irrigation District	11.6	S00E S90W	0.348 0.214
Northwest California 10/07/1951	5.8	Ferndale City Hall	56.3	S44W N46W	0.104 0.112
Kern County 06/21/1952	7.7	Pasadena - Caltech Athenaeum	127.0	S00E S90W	0.047 0.053
		Taft Lincoln School Tunnel	41.4	N21E S69E	0.156 0.179
		Santa Barbara Court House	88.4	N42E S48E	0.089 0.131
		Hollywood Storage Basement	120.4	S00W N90E	0.055 0.044
Eureka 12/21/1954	6.5	Ferndale City Hall	40.0	N44E N46W	0.159 0.201
San Francisco 03/22/1957	5.3	San Francisco Golden Gate Park	11.2	N10E S80E	0.083 0.105
Hollister 04/08/1961	5.7	Hollister City Hall	22.1	S01W N89W	0.065 0.179
Borrego Mountain 04/08/1968	6.4	El Centro Valley Irrigation District	67.3	S00W S90W	0.130 0.057
Long Beach 03/10/1933	6.3	Vernon CMD Bldg.	50.5	S08W N82W	0.133 0.155
Lower California 12/30/1934	7.1	El Centro Valley Irrigation District	66.4	S00W S90W	0.160 0.182
Helena Montana 10/31/1935	6.0	Helena, Montana Carrol College	6.2	S00W S90W	0.146 0.145
1st Northwest California 09/11/1938	5.5	Ferndale City Hall	55.2	N45E S45E	0.144 0.089
Northern California 09/22/1952	5.2	Ferndale City Hall	43.1	N44E S46E	0.054 0.076
Wheeler Ridge, California 01/12/1954	5.9	Taft Lincoln School Tunnel	42.8	N21E S69E	0.065 0.068
Parkfield, California 06/27/1966	5.6	Chalome, Shandon, California Array # 5	56.1	N05W N85E	0.355 0.434
		Cholame, Shandon, California Array # 12	53.6	N50E N40W	0.053 0.064
		Temblor, California # 2	59.6	N65W S25W	0.269 0.347

Earthquake records (continued)

Earthquake	Mag.	Station Name	Source Distance (km)	Comp.	Peak Accel. (g)
San Fernando 02/09/1971	6.4	Pacoima Dam	7.3	S16E S74W	1.172 1.070
		8244 Orion Blvd. Los Angeles, California	21.1	N00W S90W	0.255 0.134
		250 E First Street Basement, Los Angeles	41.4	N36E N54W	0.100 0.125
		Castaic Old Ridge Route	29.5	N21E N69W	0.315 0.270
		7080 Hollywood Blvd. Basement, Los Angeles	33.5	N00E N90E	0.083 0.100
		Vernon CMD Bldg.	48.0	N83W S07W	0.107 0.082
		Caltech Seismological Lab., Pasadena	34.6	S00W S90W	0.089 0.193
Loma Prieta 10/17/1989	7.1	Corralitos - Eureka Canyon Road	7.0	90 deg. 0 deg.	0.478 0.630
		Capitola - Fire Station	9.0	90 deg. 0 deg.	0.398 0.472
		Foster City - Redwood Shores	63.0	90 deg. 0 deg.	0.283 0.258
		Monterey - City Hall	49.0	90 deg. 0 deg.	0.062 0.070
		Woodside - Fire Station	55.0	90 deg. 0 deg.	0.081 0.081
Northridge 01/17/1994	6.7	Arleta Nordhoff Ave. - Fire Station	9.9	90 deg. 360 deg.	0.344 0.308
		New Hall - LA County Fire Station	19.8	90 deg. 360 deg.	0.583 0.589
		Pacoima Dam - Down Stream	19.3	265 deg. 175 deg.	0.434 0.415
		Santa Monica - City Hall Grounds	22.5	90 deg. 360 deg.	0.883 0.370
		Sylmar - County Hospital Parking Lot	15.8	90 deg. 360 deg.	0.604 0.843

APPENDIX B. MEAN AND STANDARD DEVIATIONS FOR COMPUTED RESPONSE RATIOS

Figures B.1 to B.3 present the mean and mean ± standard deviation for the response ratios computed in Section 4 using the 72 earthquake records shown in Appendix A. The figures are shown for periods ranging from 0.1 s to 4.0 s and for damping ratios of 0.02, 0.10, and 0.30. Figure B.1 shows that the scatter in the displacement response ratio data is reasonable for all periods and damping ratios. Figure B.2, however, indicates that there is much scatter in the acceleration response ratio with increased periods and damping ratios. Similar trend can also be observed for the ratio of spectral velocity to pseudo-velocity data, Figure B.3.
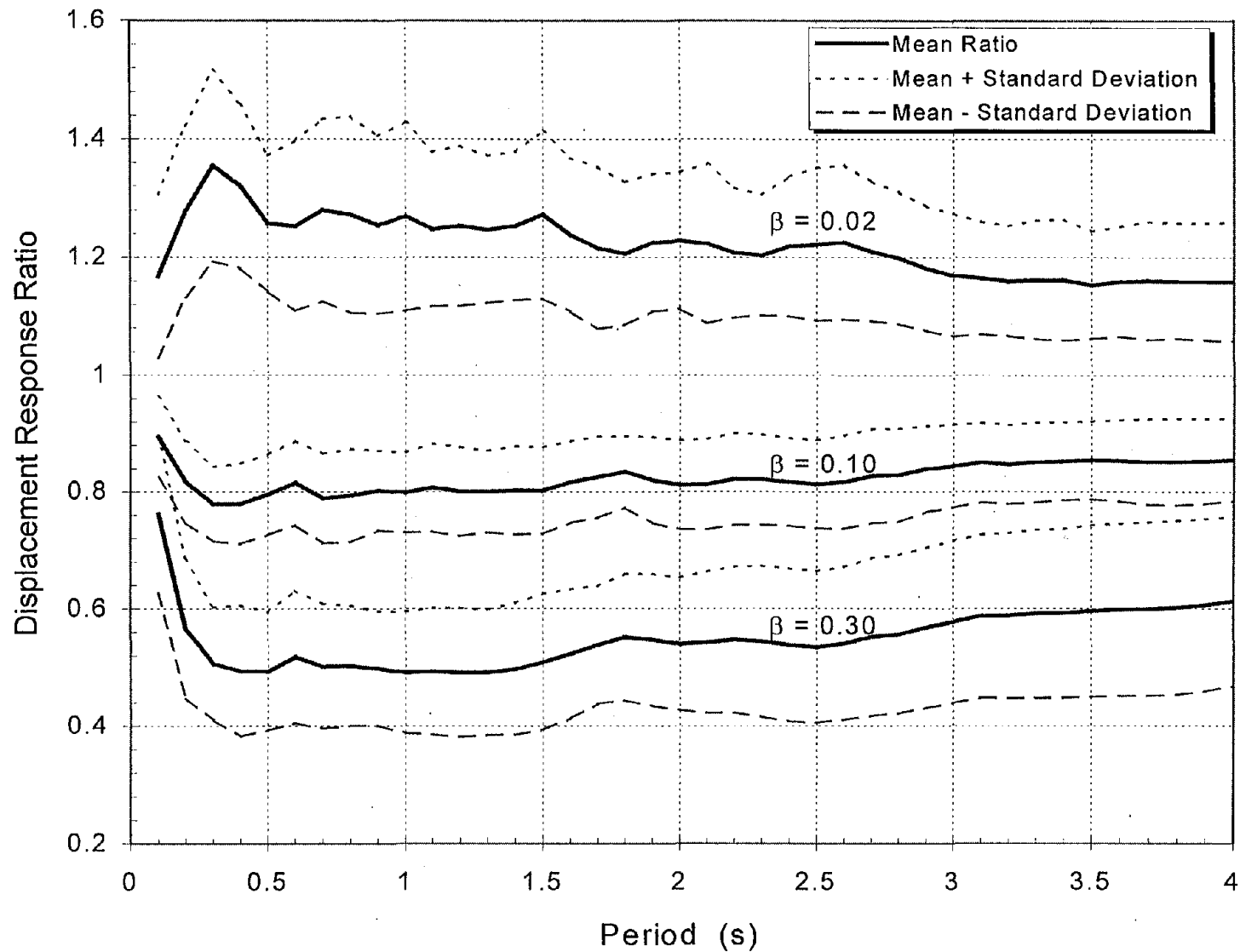
Figure B.1. Mean and Mean ± Standard Deviation of Displacement Response Ratios for SDOF Structures with Supplemental Damping
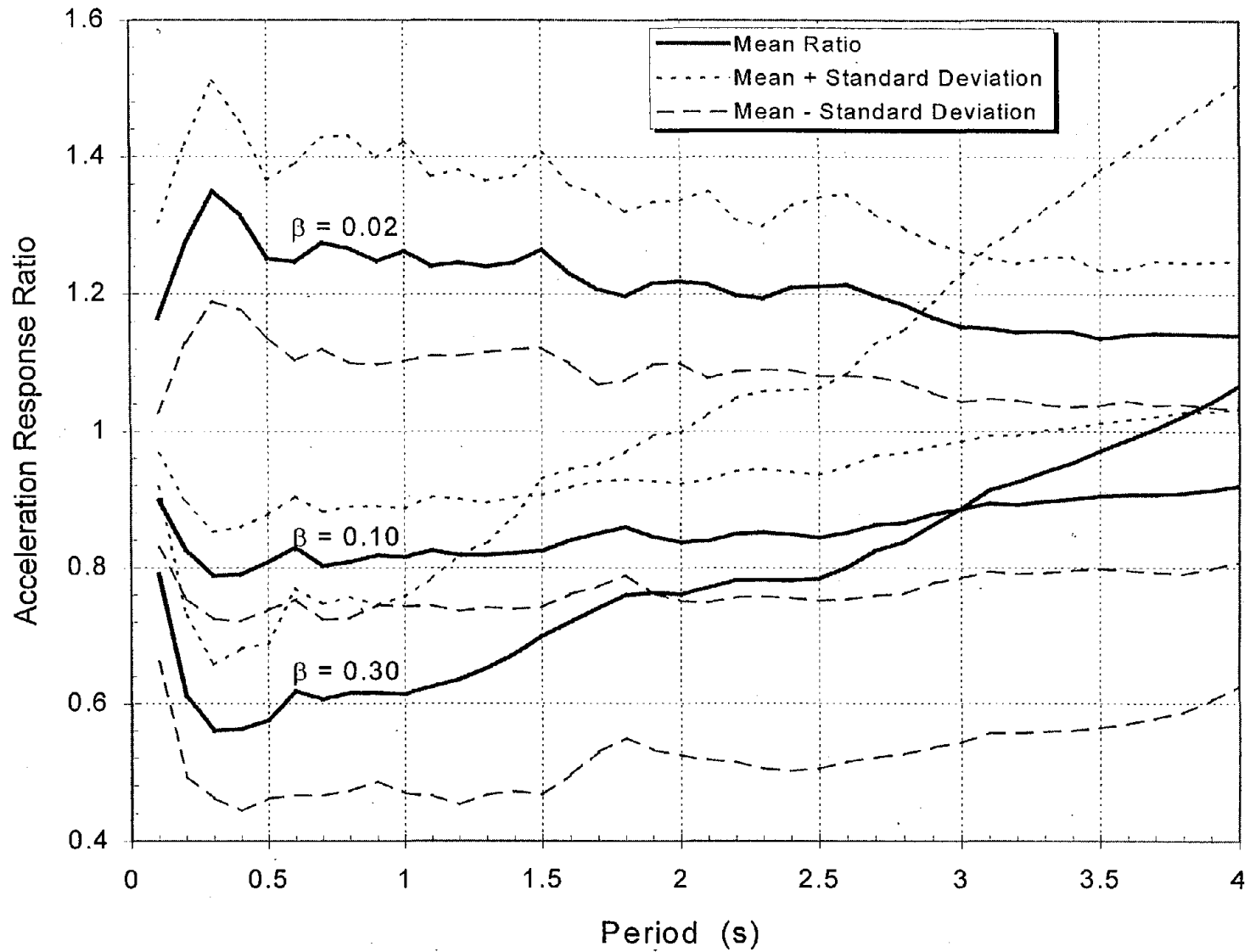
Figure B.2. Mean and Mean ± Standard Deviation of Acceleration Response Ratios for SDOF Structures with Supplemental Damping
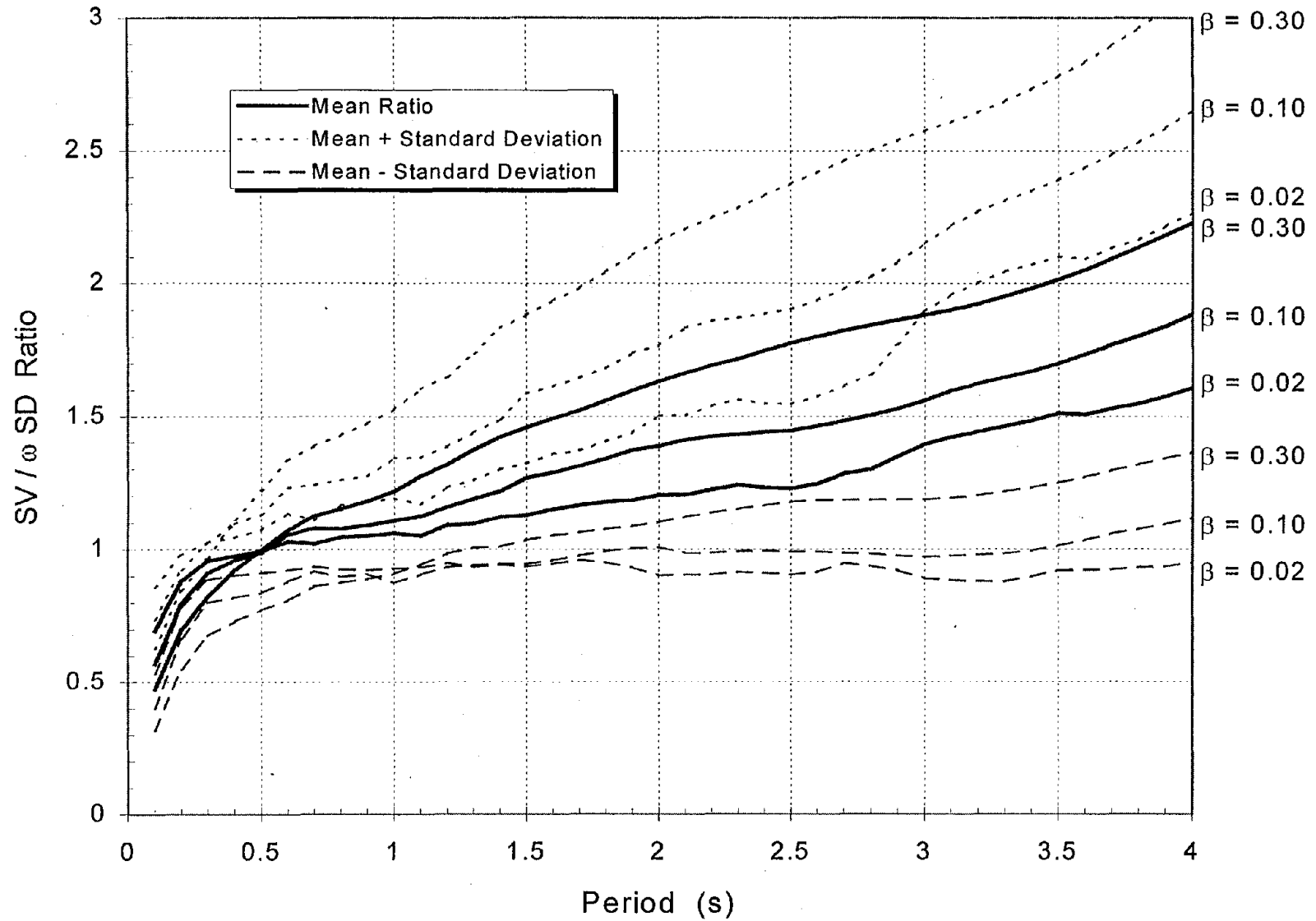
Figure B.3. Mean and Mean ± Standard Deviation of Spectral Velocity to Pseudo-Velocity Ratios for SDOF Structures with Supplemental Damping